

Mobility-Aware Performance in Hybrid RF and Terahertz Wireless Networks

Md Tanvir Hossan, *Member IEEE* and Hina Tabassum, *Senior Member IEEE*

Abstract—Using tools from stochastic geometry, this paper develops a tractable framework to analyze the performance of a mobile user in a two-tier wireless network operating on sub-6GHz and terahertz (THz) transmission frequencies. Specifically, using an equivalence distance approach, we characterize the overall handoff (HO) probability in terms of the horizontal and vertical HO and mobility-aware coverage probability. In addition, we characterize novel coverage probability expressions for THz network in the presence of molecular absorption noise and highlight its significant impact on the users’ performance. Specifically, we derive a novel closed-form expression for the Laplace Transform of the cumulative molecular noise and interference observed by a mobile user in a hybrid RF-THz network. Furthermore, we provide a novel approximation to derive the conditional distance distributions of a typical user in a hybrid RF-THz network. Finally, using the overall HO probability and coverage probability expressions, the mobility-aware probability of coverage has been derived in a hybrid RF-THz network. Our mathematical results validate the correctness of the derived expressions using Monte-Carlo simulations. The results offer insights into the adverse impact of users’ mobility and molecular noise in THz transmissions on the probability of coverage of mobile users. Our results demonstrate that a small increase in the intensity of terahertz base-stations (TBSs) (about 5 times) can increase the HO probability much more compared to the case when the intensity of RF BSs (RBSs) is increased by 100 times. Furthermore, we note that high molecular absorption can be beneficial (in terms of minimizing interference and molecular noise) for specific deployment intensity of TBSs and the benefits can outweigh the drawbacks of signal degradation due to molecular absorption.

Index Terms—Terahertz, horizontal and vertical handoff, molecular absorption noise, mobility, user association, hand-off probability, coverage probability, stochastic geometry.

I. INTRODUCTION

Connected and autonomous vehicles (CAVs) are becoming crucial nowadays to improve the driving safety, ameliorate travel efficiency through efficient parking and routing, and minimize traffic congestion. In this context, ultra-reliable and low latency communication (URLLC) is necessary to enable the exchange of real-time information between vehicles, and vehicle to infrastructure; thereby enabling vehicles (or drivers) to make informed decisions. However, unfortunately, while the conventional sub-6GHz network benefits from strong transmission powers and wider coverage zones, it may not guarantee URLLC due to extremely limited and congested spectrum. In the sequel, transmissions at millimeter-wave (mmWave) ($\sim 30 - 100\text{GHz}$) and terahertz (THz) ($\sim 0.1 - 10 \text{ THz}$)

frequencies will complement traditional wireless transmissions at sub-6GHz (or radio frequency (RF)) to support ubiquitous vehicular communications.

To date, the THz spectrum which lies in between the mmWave and the optical spectrum has been investigated rarely. However, with the recent innovations in THz signal generation, radiation, and modulation methods, the so-called THz gap is closing. THz spectrum can support massive data rates in the order of hundreds of Gigabits-per-second (Gbps), massive connectivity, and extremely secure transmissions. Nevertheless, THz channel propagation is susceptible to unique challenges such as molecular absorption noise¹, varying molecular absorption coefficients at different frequencies, and a sophisticated Beer’s Lambert law-based channel propagation model.

While THz transmissions suffer from unfavorable propagation and atmospheric absorption; there are several reasons to explore THz bands for mobility-based applications as also noted in [1], [2], i.e., **(i)** even if users are mobile, very high data rate transmission links become nearly static from the data viewpoint, i.e., the transmissions become almost “instantaneous.” In other words, although users’ channel characteristics can vary over time, the variations happen at a much slower rate than the actual data rate transmission [1], **(ii)** Even with the intermittent connectivity of a mobile user (e.g., a vehicle connecting to nearby access points), the amount of data that can be transmitted per connection is huge (i.e., 1 trillion bits in 1 second) [1], [2]. Thus, with faster communication, it is not necessary to be connected all the time. As long as the high-speed connection is available every now and then, the users can transfer or request all the data [2], **(iii)** by moving to higher carrier frequencies, the impact of Doppler effect can be minimized which is crucial for transmissions to trains/aircrafts moving at high speeds.

A. Background Work

To date, a variety of research papers analyzed the coverage performance considering a stand-alone THz network [3]–[6]. In [3], the authors characterized the average interference in a stand-alone THz network by applying the methods from the stochastic geometry assuming an interference-limited regime. However, the average interference expression was not applied to the coverage or outage analysis of a typical user. Instead, the interference distribution was approximated with a log-logistic distribution to compute the coverage probability. The authors highlighted that the application of the log-logistic

Md Tanvir Hossan and H. Tabassum are with the Department of Electrical Engineering and Computer Science, York University, (e-mail: mthossan@ieee.org, hinat@yorku.ca). This work is supported by the Discovery Grant from the Natural Sciences and Engineering Research Council of Canada.

¹A part of electromagnetic energy gets transformed into the internal energy of molecules, referred to as molecular absorption noise which is a function of frequency.

approximation may not always be precise. In [4], the authors considered a stand-alone THz network to calculate the end-to-end latency and reliability, while assuming a Gaussian distribution of the interference. Likewise, in [5], the interference was approximated with the average interference.

The aforementioned research works examined the stand-alone THz networks performance. Recently, a mixed THz and RF decode-and-forward relaying system was studied in [7]. The authors derived the cumulative density function (CDF) of the receiver's end-to-end (E2E) signal-to-noise ratio (SNR), the outage probability, and symbol error rate (SER). The authors in [8] derived the approximate coverage probability for a single-tier network, where RBS or TBS can be used in an opportunistic manner. However, given the small coverage of THz transmissions, it is practical to consider a two-tier network with a separate deployment of TBSs which is likely much denser than the deployment of RBSs. Different from the existing research, [9] characterized the exact coverage probability and interference statistics of users in a stand-alone THz network and a hybrid two-tier RF-THz network with the help of stochastic geometry.

None of the research works analyzed the impact of mobility on the performance of THz networks or multi-band networks. Also, the impact of molecular absorption noise was not considered in the stochastic-geometry based coverage analysis.

To date, several interesting research works have considered the impact of mobility in RF [10]–[12], or mm-wave networks [13]–[17]. In [10], the HO probability analysis was conducted in a multi-tier cellular network. The authors showed that there is an impact of users' mobility on tier association and coverage probability. Nevertheless, the framework in [10] only deals with the horizontal HO (i.e., the HO between the BSs in the same tier). This shortcoming arises because the closest BS to the user after HO is always considered as the new serving BS, which is not true in multi-tier networks with BSs having distinct powers, coverage zones, and operating frequencies. To overcome this shortcoming, in [11], [12], the authors applied an equivalence-based approach to analyze both the vertical and horizontal HO probabilities in a two-tier RF network. Nevertheless, to attain high speed connectivity and URLLC in 6G, it is imperative to understand the impact of mobility in multi-band wireless networks. Interestingly, in [17], the authors introduce a software defined network (SDN) switching framework for vehicles equipped with transceivers capable of dynamically switching between THz and mmWave bands to accommodate asymmetric uplink/downlink communication.

B. Motivation and Contributions

None of the research works presented a systematic stochastic geometry framework where the *equivalent distance approach* has been applied to characterize the horizontal handoff and vertical handoff probabilities (or rate)², and mobility-aware coverage probability of a user in a two-tier *multi-*

band network operating on different frequencies. Furthermore, characterizing the aforementioned performance metrics in the presence of THz transmissions brings additional novelty due to the unique features of THz that are *different from conventional RF and mm-wave*, such as (i) *molecular absorption noise* in the SINR expression, and a (ii) sophisticated *Beer's Lambert law-based channel propagation* model. To this end, the contributions of this paper are:

- We characterize the overall HO probability (which is based on the vertical and horizontal HO probability) of a mobile user in the downlink of a hybrid RF-THz network, considering the maximum received signal power association criterion. In this context, we apply an *equivalence distance approach* to facilitate the analysis of vertical HO, i.e., by introducing a virtual tier with the serving tier of a mobile user. In addition, we pointed out that a correction factor is missing in the HO probability expressions of all aforementioned research works (whether single-tier or multi-tier) related to mobility [10]–[12].
- We analyze the exact coverage probability of a typical user in the THz networks considering the repercussions of molecular noise absorption and highlight the devastating impact of ignoring the molecular absorption noise on the coverage probability. Specifically, we derive a new closed-form expression for the Laplace Transform (LT) of the cumulative molecular noise and interference observed by a typical user in THz network.
- We provide a novel approximation to derive the conditional distance distribution of a typical user in a hybrid network. To tackle mathematically challenging Beer's Lambert transmission model, we propose a novel and efficient approximation to make the framework tractable.
- Using the overall HO probability and coverage probability, we derive the *mobility-aware probability of coverage* of a mobile user in a hybrid RF-THz network.
- We provide an asymptotic closed-form expression of association probability for low molecular absorption coefficient, and asymptotic single-integral expression of no HO probability when the users move in a straight line.
- Numerical results validate the accuracy of our derived expressions. The derived expressions can be computed numerically using standard mathematical software such as MAPLE and Mathematica to obtain useful insights related to the user's performance in a hybrid RF/THz network with mobility and molecular absorption noise.

The rest of the paper is organized as follows. Section II presents the system model, assumptions, and the methodology of analysis. The horizontal and vertical HO probability analysis is presented in Section III. Section IV characterizes the coverage probability of a user in the presence of molecular absorption noise and incorporates the impact of horizontal and vertical HO probability in the calculation of the mobility-aware coverage probability. Finally, selected numerical and simulation results are presented in Section V before conclusions in Section VI.

²There are two definitions of the *HO rate* that exist in the literature. In [18], the HO rate is the ratio of the average number of cells a mobile user traverses to the average transition time (including the pause time). In [10], the HO rate is defined as the probability that the user crosses over to the next cell in one movement period. In this paper, we use the definition in [10].

Table I
LIST OF NOTATIONS

Symbol	Description	Symbol	Description
Φ_R	Locations of the conventional RBSs	R_{th}	Desired target rate
Φ_T	Locations of the conventional TBSs	θ	Boresight direction angle
Φ_u	Locations of the user	w_q	Main lobe beam-width
λ_R	Intensity of RBS	G_{max}^q	Beamforming gains of main lobes
λ_T	Intensity of TBS	G_{min}^q	Beamforming gains of side lobes
λ_u	Intensity of user	N_T	Noise originates from thermal and molecular absorption
P_R^{tx}	Transmit power of the RBSs	N_0	Thermal noise
G_R^{tx}	Transmitting antenna gain RF	r_0	Distance between the mobile user to the serving RBS
G_R^{rx}	Receiving antenna gain of RF	r_i	Distance between the i -th interfering RBS and user
c	Speed of the electromagnetic wave	r_T	Distance between initial location of the user and TBS
f_R	RF carrier frequency (in GHz)	R_T	Distance between final location of the user and TBS
α	Path-loss exponent for the RF signal	r_R	Distance between initial location of the user and RBS
H	Fading channel power	R'_R	Distance between final location of the user and RBS
N_R	Thermal noise	r'_T	Equivalent distance of r_R
I_R	cumulative interference from interfering RBSs	R'_T	Equivalent distance of R_R
H_i	Fading from the i -th interfering RBS	r'_R	Equivalent distance of r_T
P_T^{tx}	Transmit power of the TBSs	R'_R	Equivalent distance of R_T
G_T^{tx}	Transmitting antenna gain of TBSs	A_R	Association probability of a user with RBS
G_T^{rx}	Receiving antenna gain of TBSs	A_T	Association probability of a user with TBS
f_T	Carrier frequency in THz	$\mathbb{P}(H)$	Overall HO probability of the typical user
$K_a(f_T)$	Molecular absorption coefficient	v	Typical user velocity

II. NETWORK MODEL AND ASSUMPTIONS

In this section, we present the spatial network deployment model, channel propagation models, and mobility/HO model of a typical mobile user in a multi-band network. Finally, we present the step-by-step methodology of analyzing the mobility-aware coverage probability.

A. Spatial Network Deployment

A two-tier downlink network comprised of a layer of RF BSs (RBSs) and a layer of THz BSs (TBSs) is considered. The spatial deployment of the RBSs and TBSs is taken as a two-dimensional (2D) homogeneous Poisson Point Processes (PPP) Φ_R and Φ_T with intensities λ_R and λ_T , respectively. We evaluate the performance of a mobile user who is originally found at the origin and measures the channel quality from RBSs and TBSs as is done in the existing heterogeneous networks (HetNets). Users then handoff opportunistically to the RBS or TBS and the BS serves various users in orthogonal channels or time slots. The mobile user connects to a given BS based on maximum received signal power. An illustration of the considered network is shown in Fig. 1 where the typical mobile user can be classified according to its velocity, e.g., pedestrians with low velocity and vehicles with moderate to high velocity.

B. Mobility Model and HO Criterion

The typical mobile user moves with a velocity v from the origin in an arbitrary direction, thereby HO may occur depending on the maximum received signal power criterion. HOs (or association of users) can be performed based on both the instantaneous received power [19], [20] and maximum long-term averaged received power [21]–[25]. However, the short-term instantaneous fading can yield unnecessary HOs, that is, the ‘‘ping-pong effect’’. To overcome this undesired

phenomenon, the received signal power is averaged over the measurement period in long-term evolution (LTE). This assumption, also has been considered in other research works [22]–[25] and is considered as more realistic compared to instantaneous received power based user association [25, page1]. The HOs in the same tier (e.g., RBS-RBS or TBS-TBS) are referred to as *horizontal HO*. Alternatively, when the type of user switches its BSs in two different tiers (e.g., RBS-TBS or TBS-RBS), then this HO is referred to as *vertical HO*.

C. RF and THz Communication Model

1) *RF Model*: The signal transmitted from RBS incurs path-loss and short-term fading which is Rayleigh distributed. At the typical mobile user, the received signal power is defined as:

$$P_R^{rx} = G_R^{tx} G_R^{rx} \left(\frac{c}{4\pi f_R} \right)^2 \frac{P_R^{tx}}{r_0^\alpha}, \quad (1)$$

The signal-to-interference-plus noise ratio (SINR) of a typical mobile user on RF transmission channel is thus modeled as:

$$\text{SINR}_R = \frac{P_R^{tx} G_R^{tx} G_R^{rx} \left(\frac{c}{4\pi f_R} \right)^2 H}{r_0^\alpha (N_R + I_R)} = \frac{P_R^{tx} \gamma_R H}{r_0^\alpha (N_R + I_R)}, \quad (2)$$

where P_R^{tx} , G_R^{tx} , G_R^{rx} , c , f_R , r_0 , and α denote the transmit power from the RBSs, transmitting antenna gain, receiving antenna gain, speed of the electromagnetic wave, RF carrier frequency (in GHz), distance between the mobile user to the serving RBS, and path-loss exponent of the signal, respectively. Also, H is the exponentially distributed channel fading power of the mobile user from the targeted RBS, N_R is the power of thermal noise at the receiver, $I_R = \sum_{i \in \Phi_R \setminus 0} P_R^{tx} \gamma_R r_i^{-\alpha} H_i$ is the cumulative interference at the mobile user from the interfering RBSs. From the cumulative interference, r_i is the distance between the i -th interfering

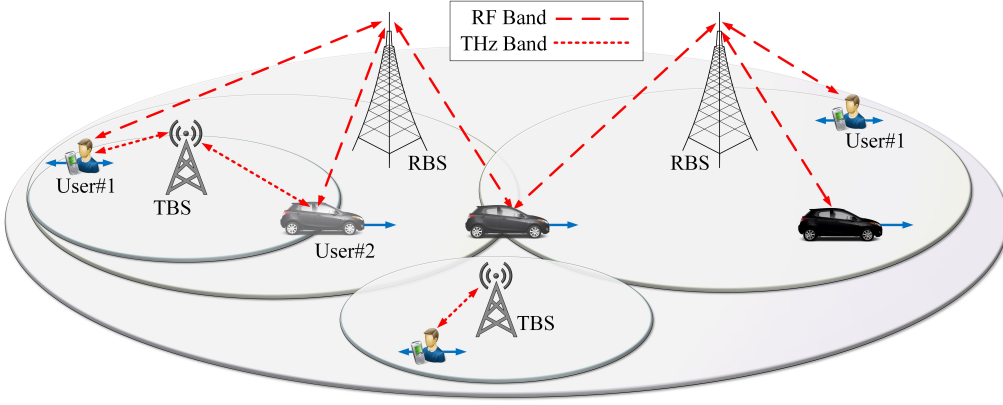


Figure 1. Graphical illustration of a two-tier hybrid RF-THz network with low- and high-velocity users.

RBS and the typical mobile user, H_i is the power of fading from the i -th interfering RBS to the typical mobile user, and $\gamma_R = G_R^{\text{tx}} G_R^{\text{rx}} (c/4\pi f_R)^2$.

2) *THz Model*: In THz network, the line-of-sight (LOS) transmissions are much more significant than the non-line-of-sight (NLOS) transmissions due to the presence of molecular absorption. Subsequently, in this work, following [1], [3], [4], we calculate the received power taking into account the LOS transmission property from [26], [9] as follows³:

$$P_T^{\text{rx}} = G_T^{\text{tx}} G_T^{\text{rx}} \left(\frac{c}{4\pi f_T} \right)^2 \frac{P_T^{\text{tx}} \exp(-K_a(f_T) d_0)}{d_0^2}, \quad (3)$$

where P_T^{tx} , G_T^{tx} , G_T^{rx} , f_T , d_0 , and $K_a(f_T)$ denote the transmit power of the TBSs, transmitting antenna gain of the TBS, receiving antenna gain of the TBS, THz carrier frequency, distance between the mobile user to the serving TBS, and the molecular absorption coefficient depends on the composition of the medium and also on the frequency (i.e., f_T) of the signal, respectively. For any specific THz carrier frequency f_T , $K_a(f_T)$ ⁴ can be calculated as follows [29]:

$$K_a(f_T) = \sum_{(i,g)} \frac{p^2 T_{\text{sp}} q^{(i,g)} N_A S^{(i,g)} f \tanh\left(\frac{hc f}{2k_b T}\right)}{p_0 V T^2 f_c^{(i,g)} \tanh\left(\frac{hc f_c^{(i,g)}}{2k_b T}\right)} F^{(i,g)}(f), \quad (4)$$

where p and p_0 are the ambient pressure of the transmission medium and the reference pressure, respectively, T is the temperature of the transmission medium, T_{sp} is the temperature at standard pressure, $q^{(i,g)}$ indicates the mixing ratio of the isotopologue i of gas g , N_A refers to the Avogadro number, and V is the gas constant. The line intensity $S^{(i,g)}$ defines the strength of the absorption by a specific type of molecules and is directly obtained from the HITRAN database [30]. In addition, f and $f_c^{(i,g)}$ denote the THz frequency and the resonant frequency of gas g , respectively, c is the speed of light, h is the Planck's constant, and k_b is the Boltzmann

³THz transmissions are prone to the the molecular absorption in the (indoor/outdoor) atmosphere. This absorption process can be described with the help of *Beer-Lambert's law* which states that the amount of radiation that is able to propagate from a transmitter to the receiver through the absorbing medium can be characterized by $\exp(-K_a(f_T) d_0)$, where $K_a(f_T)$ denotes the molecular absorption coefficient of the indoor or outdoor medium [27], [28]. The model is shown to be applicable to both indoor and outdoor scenarios [27], [28]. Our contributions in this paper are general and are applicable for any values of $K_a(f_T)$.

⁴For the sake of brevity, we will drop the argument of $K_a(f_T)$ from this point onwards in the paper.

constant. For the frequency f , we consider the Van Vleck-Weisskopf asymmetric line shape to evaluate:

$$F^{(i,g)}(f) = \frac{100 c \alpha^{(i,g)} f}{\pi f_c^{(i,g)}} \left(\frac{1}{Y^2 + (\alpha^{(i,g)})^2} + \frac{1}{Z^2 + (\alpha^{(i,g)})^2} \right),$$

where $Y = f + f_c^{(i,g)}$ and $Z = f - f_c^{(i,g)}$, and the Lorentz half-width is given as follows:

$$\alpha^{(i,g)} = \left((1 - q^{(i,g)}) \alpha_{\text{air}}^{(i,g)} + q^{(i,g)} \alpha_0^{(i,g)} \right) \left(\frac{p}{p_0} \right) \left(\frac{T_0}{T} \right)^\gamma,$$

where T_0 is the reference temperature, the parameters air half-widths, $\alpha_{\text{air}}^{(i,g)}$, self-broadened half-widths, $\alpha_0^{(i,g)}$, and temperature broadening coefficient, γ , are obtained from the HITRAN database [30]. The resonant frequency of gas g at reference pressure p_0 is determined as $f_c^{(i,g)} = f_{c_0}^{(i,g)} + \delta^{(i,g)} \left(\frac{p}{p_0} \right)$, where $\delta^{(i,g)}$ is the linear pressure shift [29].

Note that $G_T^{\text{tx}}(\theta_q)$ as well as $G_T^{\text{rx}}(\theta_q)$ are directional transmitter and receiver antenna gains, respectively. The beamforming gains from the main lobe and side lobes of the TBS transmitting antenna can be generalized as follows [31]:

$$G_T^q(\theta) = \begin{cases} G_{\text{max}}^q & |\theta_q| \leq w_q \\ G_{\text{min}}^q & |\theta_q| > w_q \end{cases}, \quad (5)$$

where $q \in \{\text{tx}, \text{rx}\}$, $\theta_q \in [-\pi, \pi)$ is the angle off the boresight direction, w_q is the beamwidth of the main lobe, G_{max}^q and G_{min}^q are the beamforming gains of the main and side lobes, respectively. We assume that the typical mobile user's receiving beam aligns with the transmitting beam of the associated TBS through beam alignment techniques. However, for the alignment between the user and interfering TBSs, we define a random variable D , which can take values as $D \in \{G_{\text{max}}^{\text{tx}} G_{\text{max}}^{\text{rx}}, G_{\text{max}}^{\text{tx}} G_{\text{min}}^{\text{rx}}, G_{\text{min}}^{\text{tx}} G_{\text{max}}^{\text{rx}}, G_{\text{min}}^{\text{tx}} G_{\text{min}}^{\text{rx}}\}$, and the respective probability for each case is $F_{\text{tx}} F_{\text{rx}}$, $F_{\text{tx}}(1 - F_{\text{rx}})$, $(1 - F_{\text{tx}}) F_{\text{rx}}$, and $(1 - F_{\text{tx}})(1 - F_{\text{rx}})$, where $F_{\text{tx}} = \frac{\theta_{\text{tx}}}{2\pi}$ and $F_{\text{rx}} = \frac{\theta_{\text{rx}}}{2\pi}$, respectively. Assuming that the main lobe of the typical mobile user's receiver is coinciding with that of its

desired TBS⁵, its SINR can be formulated as follows:

$$\begin{aligned} \text{SINR}_T &= \frac{G_T^{\text{tx}} G_T^{\text{rx}} \left(\frac{c}{4\pi f_T} \right)^2 P_T^{\text{tx}} \exp(-K_a d_0) d_0^{-2}}{N_T + I_T}, \\ &= \frac{\gamma_T P_T^{\text{tx}} \exp(-K_a d_0) d_0^{-2}}{N_T + I_T}, \end{aligned} \quad (6)$$

where $I_T = \sum_{i \in \Phi_T \setminus 0} \gamma_T P_T^{\text{tx}} F d_i^{-2} \exp(-K_a d_i)$ is the cumulative interference at the mobile user, d_i is the distance of the that user to the i -th interfering TBS, $F = F_{\text{tx}} F_{\text{rx}} = \frac{\theta_{\text{tx}} \theta_{\text{rx}}}{4\pi^2}$ is the probability of alignment between the main lobes of the interferer and the typical user assuming negligible side-lobe gains and $\gamma_T = G_T^{\text{tx}} G_T^{\text{rx}} c^2 / (4\pi f_T)^2$. The cumulative thermal and molecular absorption noise is [33], [4], [34]:

$$\begin{aligned} N_T &= N_0 + P_T^{\text{tx}} \gamma_T d_0^{-2} (1 - e^{-K_a d_0}) + \\ &\quad \sum_{i \in \Phi_T \setminus 0} \gamma_T F P_T^{\text{tx}} d_i^{-2} (1 - \exp(-K_a d_i)). \end{aligned} \quad (7)$$

Note that the internal vibration of the molecules re-emit a part of the absorbed energy back to the channel resulting in the so-called *molecular absorption noise* [29], [35], [36]. The molecular absorption noise is induced by the transmissions of the users sharing the same frequency. As such, the second and third terms in N_T represent the molecular absorption noise due to the desired users' transmission and the interfering users' transmission, respectively. The SINR from TBS can then be modeled as follows:

$$\text{SINR}_T = \frac{P_T^{\text{tx}} \gamma_T d_0^{-2} e^{-K_a d_0}}{N_0 + P_T^{\text{tx}} \gamma_T d_0^{-2} (1 - e^{-K_a d_0}) + \sum_{i \in \Phi_T \setminus 0} P_T^{\text{tx}} \gamma_T F d_i^{-2}}$$

The SINR expression is different from the traditional RF systems due to THz channel propagation model in the numerator and molecular noise consideration in the denominator.

D. Methodology of Analysis

The methodology of analyzing the HO probability and mobility-aware coverage probability in a multi-band network can be summarized as follows:

- Using Eq.(3), derive the conditional probability density function (PDF) of the distance of a mobile user tagged to the TBS ($f_{r_T}(r_T)$) and RBS ($f_{r_R}(r_R)$) in a multi-band network.
- Using Eq.(3), derive the conditional HO probability of a typical user who is initially associated to TBS ($\mathbb{P}(H_T)$) and initially associated to RBS ($\mathbb{P}(H_R)$).
- Using Eq.(3) and the association probabilities of the typical user to TBSs and RBSs, i.e., A_T and A_R , respectively, and conditional HO probabilities $\mathbb{P}(H_R)$ and $\mathbb{P}(H_T)$, derive the overall HO probability, i.e., $\mathbb{P}(H)$ of the typical user.
- Using Eq.(3), we derive the LT of the cumulative interference and molecular noise as well as the coverage probability of the typical user without mobility \mathbb{C} .
- Derive the coverage probability of the typical user with mobility \mathbb{C}_M .

⁵The beamforming model is based on a two-lobe approximation of the antenna pattern. Although simple, the model is tractable and capture primary features such as the directivity gain, the front-to-back ratio, and the half-power beamwidth [31], [32].

III. HO PROBABILITY IN A HYBRID RF-THZ NETWORK

In this section, first develop HO criterion from TBS and derive the conditional HO probability from TBS, i.e., $\mathbb{P}(H_T)$, which comprises of the HO probability from TBS to TBS (horizontal HO) and TBS to RBS (vertical HO). Then, we formulate and simplify the HO criterion from RBS and derive the HO probability from RBS, i.e, $\mathbb{P}(H_R)$, which comprises of the HO probability from RBS to RBS (horizontal HO) and RBS to TBS (vertical HO). Finally, develop the overall HO probability of the mobile user, which is defined as:

$$\mathbb{P}(H) = A_R \mathbb{P}(H_R) + A_T \mathbb{P}(H_T), \quad (8)$$

where A_R and A_T denote the association probabilities of a user with RBS and TBS, respectively.

From the relationship between the received powers of TBSs and RBSs, the association probability to TBS can be defined as follows:

$$\begin{aligned} A_T &= \mathbb{E}_{d_0} [\mathbb{P}(P_T^{\text{rx}} > P_R^{\text{rx}})], \\ &= \mathbb{E}_{d_0} \left[\mathbb{P} \left(P_T^{\text{tx}} \gamma_T \frac{\exp(-K_a d_0)}{d_0^2} > P_R^{\text{tx}} \gamma_R r_0^{-\alpha} \right) \right], \quad (9) \\ &\stackrel{(a)}{=} \mathbb{E}_{d_0} \left[\exp \left(-\pi \lambda_R (Q d_0^2 \exp(K_a d_0))^{\frac{2}{\alpha}} \right) \right], \end{aligned}$$

where from the null probability of PPP Φ_R and $Q = \frac{P_R^{\text{tx}} \gamma_R}{P_T^{\text{tx}} \gamma_T}$, we get step (a) in Eq. (18). This null property stated the probability that no RBSs are closer to a user than the distance z , which is $\mathbb{P}(\rho \geq z) = \exp(-\pi \lambda_R z^2)$ for given a tier of RBSs with intensity λ_R . The PDFs of the distances between the typical user and the closest RBS and TBS are given as $f_{r_0}(r_0) = 2\pi \lambda_T r_0 \exp(-\pi \lambda_T r_0^2)$ and $f_{d_0}(d_0) = 2\pi \lambda_T d_0 \exp(-\pi \lambda_T d_0^2)$, respectively. Therefore, the association probability with TBS can be achieved by averaging over d_0 .

$$A_T = \int_0^\infty \exp \left(-\pi \lambda_R Q^{\frac{2}{\alpha}} d_0^{\frac{4}{\alpha}} \exp \left(\frac{2K_a d_0}{\alpha} \right) \right) f_{d_0}(d_0) dd_0, \quad (10)$$

where $A_R = 1 - A_T$. When $\alpha = 4$ and $K_a \rightarrow 0$, a closed-form expression can be given as:

$$\begin{aligned} A_T &= \int_0^\infty \exp \left(-\pi \lambda_R Q^{\frac{2}{\alpha}} d_0^{\frac{4}{\alpha}} \right) f_{d_0}(d_0) dd_0 \\ &= 1 - 0.5 \pi \lambda_R e^{\frac{\pi Q \lambda_R^2}{4 \lambda_T}} \sqrt{\frac{Q}{\lambda_T}} \operatorname{erfc} \left(\frac{\lambda_R}{2} \sqrt{\frac{\pi Q}{\lambda_T}} \right), \end{aligned} \quad (11)$$

A. HO Probability Characterization from TBS

1) *HO Criterion from TBS*: Fig. 2(a) illustrates an outline of an user, who is initially tagged with a TBS at the position c_1 . Let r_T is the distance between the user and the tagged TBS in a hybrid RF-THz network whose PDF is given as follows.

Lemma 1. *The conditional PDF of the distance from a mobile user initially connected to TBS to the desired TBS is:*

$$f_{r_T}(r_T) = \frac{2\pi \lambda_T r_T}{A_T} \times$$

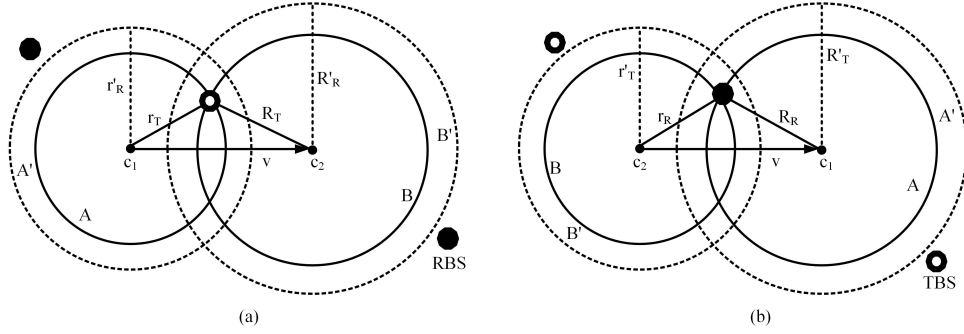


Figure 2. Graphical illustration of different HO events, (a) HO from TBS: At c_1 , a mobile user is initially associated with a TBS, where the distance between user and TBS is r_T . After HO at c_2 , the distance becomes r_R . The virtual tiers are shown by the dotted lines, i.e., the equivalent distance of the TBS from c_1 and c_2 in RF tier is represented by r'_R and R'_R , respectively. (b) HO from RBS: At c_2 , a mobile user is initially associated with a RBS, where the distance between user and RBS is r_R . After HO at c_1 , the distance becomes r_T . The virtual tiers are shown by the dotted lines, i.e., the equivalent distance of the RBS from c_2 and c_1 is represented by r'_T and R'_T , respectively.

$$\exp\left(-\pi\lambda_T r_T^2 - \pi\lambda_R (r_T^2 Q)^{\frac{2}{\alpha}} \exp\left(\frac{2K_a r_T}{\alpha}\right)\right). \quad (12)$$

Proof. See **Appendix A**. ■

The area A is centered by c_1 with radius r_T . Assume that the user moves its position from c_1 to c_2 . The new distance R_T denotes the distance between c_2 and the tagged TBS and B denotes the area centered at c_2 with radius R_T . At position c_2 , the vertical HO takes place when the maximum received power of RBS is greater than the TBS, i.e., $P_T^x < P_R^x$, which results in:

$$r_R < \exp\left(\frac{K_a r_T}{\alpha}\right) (Q r_T^2)^{\frac{1}{\alpha}} \triangleq r'_R, \quad (13)$$

From Eq. (13), we define r'_R is the equivalent distance of r_T . That is, when $r_T > r_R > r'_R$, vertical HO will not occur because it violates Eq. (13).

2) *HO Analysis:* Provided that the typical mobile user is originally tagged to TBS, the conditional HO probability from TBS can be determined by averaging over r_T and θ as follows:

$$\mathbb{P}(H_T) = 1 - \mathbb{P}(\overline{H}_T) = 1 - \mathbb{E}_{r_T, \theta}[\mathbb{P}(\overline{H}_T | r_T, \theta)]. \quad (14)$$

To derive the no HO probability ($\mathbb{P}(\overline{H}_T)$) of a typical user who is associated to TBS, we replace the serving TBS by a virtual TBS in RF tier with distance r'_R away from the target mobile user. There will be no HO if no RBSs or TBSs are closer to the user than r'_R . In Fig. 2(a), the area A' centered at c_1 with radius r'_R . Here, the THz tier is the serving tier suggests all RBSs are found outside the area A' . Likewise, B' is the area centered at c_2 with radius R'_R , which is the corresponding distance of R_T . If RBSs are not remained within the area B' , then initial TBS will remain the target BS even after the movement.

Lemma 2. *Given a mobile user is initially associated with a TBS, the conditional probability of no HO from the serving TBS in a hybrid RF-THz network finds as follows:*

$$\begin{aligned} \mathbb{P}(\overline{H}_T) &= \frac{1}{\pi} \left(\int_{\theta=0}^{\frac{\pi}{2}} \int_{r_T=0}^{\infty} f_{r_T}(r_T) e^{(-\lambda_T S_T - \lambda_R S'_T)} dr_T d\theta \right. \\ &\quad \left. + \int_{\theta=\frac{\pi}{2}}^{\pi} \int_{r_T=0}^{v \cos(\pi-\theta)} f_{r_T}(r_T) e^{(-\lambda_T C_T - \lambda_R C'_T)} dr_T d\theta \right) \end{aligned}$$

$$+ \int_{\theta=\frac{\pi}{2}}^{\pi} \int_{r_T=v \cos(\pi-\theta)}^{\infty} f_{r_T}(r_T) e^{(-\lambda_T S_T - \lambda_R S'_T)} dr_T d\theta \Big),$$

where $S_T = |B| - |B \cap A|$, $S'_T = |B'| - |B' \cap A'|$, $C_T = R_T^2(\pi - \theta_1^T) + r_T v \sin\theta - r_T^2(\pi - \theta)$, $C'_T = R_R'^2(\pi - \theta_3^T) + r'_R v \sin\theta_2^T - r_R'^2(\pi - \theta_2^T)$, $\theta_1^T = \theta - \pi + \sin^{-1}\left(\frac{v \sin\theta}{R_T}\right)$, $\theta_3^T = \theta - \pi + \sin^{-1}\left(\frac{v \sin\theta}{R'_R}\right)$.

Proof. See **Appendix B**. ■

In the following, as a special case of the aforementioned lemma, we have provided the HO probability of a mobile user when $\lambda_R \rightarrow 0$ which results in a stand-alone THz network.

Corollary 1. *As $\lambda_R \rightarrow 0$ then $A_T \rightarrow 1$, the conditional HO probability can be simplified as:*

$$\begin{aligned} \mathbb{P}(H_T) &= 1 - \frac{1}{\pi} \left(\int_{\theta=0}^{\frac{\pi}{2}} \int_{r_T=0}^{\infty} f_{d_0}(r_T) e^{-\lambda_T S_T} dr_T d\theta \right. \\ &\quad \left. + \int_{\theta=\frac{\pi}{2}}^{\pi} \int_{r_T=0}^{v \cos(\pi-\theta)} f_{d_0}(r_T) e^{-\lambda_T C_T} dr_T d\theta \right. \\ &\quad \left. + \int_{\theta=\frac{\pi}{2}}^{\pi} \int_{r_T=v \cos(\pi-\theta)}^{\infty} f_{d_0}(r_T) e^{-\lambda_T S_T} dr_T d\theta \right). \end{aligned}$$

Another special case is a situation when a mobile user moves in a straight line. In this case, **Lemma 2** can be simplified by substituting $\theta = 0$ as follows:

Corollary 2. *Given a mobile user is initially associated with a TBS and moving in a straight line, the conditional probability of no HO from the serving TBS can be given as follows:*

$$\mathbb{P}(\overline{H}_T) = \frac{1}{\pi} \int_{r_T=0}^{\infty} f_{r_T}(r_T) \exp(-\lambda_T S_T - \lambda_R S'_T) dr_T \quad (15)$$

where $S_T = \pi(R_T^2 - r_T^2)$, $S'_T = \pi R_R'^2 - r_R'^2(\pi - \theta_2^T) + r'_R v \sin\theta_2^T$, $R_T^2 = r_T^2 + v^2 + 2r_T v$, $R_R' = (R_T)^{\frac{2}{\alpha}} e^{\frac{K_a R_T}{\alpha}} \left(\frac{P_R^{tx} Q}{P_T^{tx}}\right)^{\frac{1}{\alpha}}$, $r'_R = (r_T)^{\frac{2}{\alpha}} e^{\frac{K_a R_T}{\alpha}} \left(\frac{P_R^{tx} Q}{P_T^{tx}}\right)^{\frac{1}{\alpha}}$, $\theta_2^T = \cos^{-1}\left(\frac{r_R'^2 + v^2 - R_R'^2}{2r'_R v}\right)$.

B. HO Probability Characterization from RBS

1) *HO Criterion from RBS*: Fig. 2(b) denotes a situation where a mobile user is tagged with a given RBS at the position c_2 . Given the user is associated to the RBS in a multi-band network, let r_R be the distance between the mobile user and RBS whose PDF is given below.

Lemma 3. *The PDF of the conditional distance r_R from a typical mobile user initially connected to RBS to desired RBS can be acquired as follows:*

$$f_{r_R}(r_R) = \frac{2\pi\lambda_R r_R}{A_R} \exp\left(-\pi\lambda_R r_R^2 - \pi\lambda_T \left(\frac{r_R^\alpha}{Q}\right)^{\frac{2}{2+\mu}}\right). \quad (16)$$

Proof. See **Appendix A**. ■

The area centered by c_2 with radius r_R is denoted by B . Let R_R denotes the distance between c_1 and RBS. When user moves to c_1 , the HO occurs if the maximum received power of TBS is greater than that of RF tier, i.e., $P_R^{\text{rx}} < P_T^{\text{rx}}$, which results in the following:

$$r_T^2 \exp(K_a r_T) < (r_R)^\alpha (1/Q). \quad (17)$$

Note that the exponential term is a function of r_T ; therefore, for the sake of tractability and to apply the equivalent distance approach, we approximate $r_T^\mu \approx \exp(K_a r_T)$ then, $r_T^2 \exp(K_a r_T) \approx (r_T)^{2+\mu}$. Subsequently, we have $r_T < [(r_R)^\alpha (1/Q)]^{\frac{1}{2+\mu}} \triangleq r'_T$, where μ is a correcting factor and r'_T specifies the virtual distance of r_R . That is, when $r_R > r_T > r'_T$, there will be no HO.

Choice of μ : To select μ appropriately, we calculate the probability of association of the typical mobile user to RBS by using the exact result of A_T in (10) and then equate it to the approximate association probability obtained as follows:

$$\begin{aligned} \tilde{A}_R &= \mathbb{E}_{r_0} [\mathbb{P}(P_R^{\text{rx}} > P_T^{\text{rx}})], \\ &= \mathbb{E}_{r_0} \left[\mathbb{P} \left(P_R \gamma_R r_0^{-\alpha} > P_T \gamma_T \frac{\exp(-K_a d_0)}{d_0^2} \right) \right], \\ &\approx \mathbb{E}_{r_0} \left[\mathbb{P} \left(P_R \gamma_R r_0^{-\alpha} > P_T \gamma_T d_0^{-2-\mu} \right) \right], \\ &\stackrel{(a)}{=} \mathbb{E}_{r_0} \left[\exp \left(-\pi\lambda_T \left(\frac{r_0^\alpha}{Q} \right)^{\frac{1}{2+\mu}} \right) \right], \\ &= \int_0^\infty \exp \left(-\pi\lambda_T \left(\frac{r_0^\alpha}{Q} \right)^{\frac{1}{2+\mu}} \right) f_{r_0}(r_0) dr_0. \end{aligned} \quad (18)$$

Solving $A_R = \tilde{A}_R$ gives us the appropriate value of μ . Note that when the molecular absorption coefficient $K_a \rightarrow 0$, the value of $\mu \rightarrow 0$ and the approximation becomes exact, i.e., $\tilde{A}_R = 1 - A_T$.

2) *HO Analysis*: When the typical mobile user is originally associated to THz tier, the HO probability from RBS can be determined by taking the average over r_R and θ as follows:

$$\mathbb{P}(H_R) = 1 - \mathbb{P}(\bar{H}_R) = 1 - \mathbb{E}_{r_R, \theta} [\mathbb{P}(\bar{H}_R | r_R, \theta)]. \quad (19)$$

To derive the no HO probability ($\mathbb{P}[\bar{H}_R]$) of a mobile user who is tagged to RBS, we replace the serving RBS by a virtual RBS in THz tier, therefore, the new distance is r'_T away from

the target mobile user. Fig. 2(b) shows the area B' centered at c_2 with radius r'_T . The fact that RF tier is acting as the serving tier to serve the mobile user indicates that all the other BSs of THz tier are situated outside B' . Here, the area A' with the radius R'_T , which is centered at c_1 . The radius R'_T is the equivalent distance of R_R . If no TBSs are located in the area A' , then initial RBS will remain the tagged BS even after movement of the user. There will be no HO if no RBSs or TBSs are closer than r'_T .

Lemma 4. *Given a mobile user is originally associated with a RBS, the probability of no HO from the serving RBS in a hybrid RF-THz network can be derived as follows:*

$$\begin{aligned} \mathbb{P}[\bar{H}_R] &= \frac{1}{\pi} \left(\int_{\theta=0}^{\frac{\pi}{2}} \int_{r_R=0}^{\infty} f_{r_R}(r_R) e^{(-\lambda_R S_R - \lambda_T S'_R)} dr_R d\theta \right. \\ &+ \int_{\theta=\frac{\pi}{2}}^{\pi} \int_{r_R=0}^{v \cos(\pi-\theta)} f_{r_R}(r_R) e^{(-\lambda_R C_R - \lambda_T C'_R)} dr_R d\theta \\ &\left. + \int_{\theta=\frac{\pi}{2}}^{\pi} \int_{r_R=v \cos(\pi-\theta)}^{\infty} f_{r_R}(r_R) e^{(-\lambda_R S_R - \lambda_T S'_R)} dr_R d\theta \right), \end{aligned}$$

where $S_R = |A| - |A \cap B|$, $S'_R = |A'| - |A' \cap B'|$, $C_R = R_R^2(\pi - \theta_1^R) + r_R v \sin\theta - r_R^2(\pi - \theta)$, $C'_R = R_T^2(\pi - \theta_3^R) + r'_T v \sin\theta_2^R - r_T^2(\pi - \theta_2^R)$, $\theta_1^R = \theta - \pi + \sin^{-1} \left(\frac{v \sin\theta}{R_R} \right)$, $\theta_3^R = \theta - \pi + \sin^{-1} \left(\frac{v \sin\theta}{R'_T} \right)$.

Proof. See **Appendix C**. ■

Another special case is a situation when a mobile user moves in a straight line. In this case, **Lemma 4** can be simplified by substituting $\theta = 0$ as follows:

Corollary 3. *Given a mobile user is initially associated with a RBS and moving in a straight line, the conditional probability of no HO from the serving RBS can be given as follows:*

$$\mathbb{P}[\bar{H}_R] = \frac{1}{\pi} \int_{r_R=0}^{\infty} f_{r_R}(r_R) \exp(-\lambda_R S_R - \lambda_T S'_R) dr_R \quad (20)$$

where $S_R = \pi(R_R^2 - r_R^2)$, $S'_R = \pi R_T^2 - r_T^2(\pi - \theta_2^R) + r'_T v \sin\theta_2^R$, $R_R^2 = r_R^2 + v^2 - 2r_R v \cos(\pi - \theta) = r_R^2 + v^2 + 2r_R v$, $R'_T = \left[(R_R)^\alpha \left(\frac{P_T^{\text{tx}}}{P_R^{\text{tx}} Q} \right) \right]^{\frac{1}{2+\mu}}$, $r'_T = \left[(r_R)^\alpha \left(\frac{P_T^{\text{tx}}}{P_R^{\text{tx}} Q} \right) \right]^{\frac{1}{2+\mu}}$, $\theta_2^R = \cos^{-1} \left(\frac{r_T^2 + v^2 - R_T^2}{2r_T v} \right)$.

C. Overall HO Probability

The HO probability of a mobile user in a hybrid RF-THz network finds as follows:

$$\mathbb{P}(H) = A_R \mathbb{P}(H_R) + A_T \mathbb{P}(H_T) = 1 - A_R \mathbb{P}(\bar{H}_R) - A_T \mathbb{P}(\bar{H}_T), \quad (21)$$

where A_R and A_T are given in (10). Likewise, $\mathbb{P}(\bar{H}_T)$ and $\mathbb{P}(\bar{H}_R)$ are given by **Lemma 2** and **Lemma 4**, respectively.

IV. COVERAGE PROBABILITY WITH AND WITHOUT MOBILITY

In this section, first we characterize the conditional coverage probabilities from TBS and RBS, i.e., \mathbb{C}_T and \mathbb{C}_R , respectively.

Then, the probability of coverage with and without mobility will be derived. Since a mobile user can connect to either RF or THz tier, the unconditional probability of coverage without mobility can demonstrate as follows:

$$\mathbb{C} = A_T \mathbb{C}_T + A_R \mathbb{C}_R, \quad (22)$$

where A_T and A_R are defined in Section III. Here, the TBSs and RBSs are distributed as different PPPs, therefore, the distance of a typical mobile user to its serving BS depends on the associated tier. Afterwards, the PDF of the conditional distance of the typical mobile user to TBS and RBS can be given as in **Lemma 1** and **Lemma 3**, respectively.

A. Conditional Coverage Probability - THz

Conditioned on the fact that the mobile user is tagged to TBS, the conditional rate coverage probability is defined as the probability of this user achieving a target data rate R_{th} . Using $R_{\text{th}} = W_T \log_2(1 + \text{SINR}_T)$ (where W_T is the bandwidth for THz transmission), the conditional rate coverage probability is given below:

$$\begin{aligned} \mathbb{C}_T &= \mathbb{P}\left(\text{SINR}_T > 2^{\frac{R_{\text{th}}}{W_T}} - 1\right) = \mathbb{P}(\text{SINR}_T > \tau_T), \\ &= \mathbb{P}\left(\frac{P_T^{\text{tx}} \gamma_T(r_{T,0})^{-2} \left((1 + \tau_T) e^{-K_a r_{T,0}} - \tau_T\right)}{N_0 + \sum_{i \in \Phi \setminus 0} P_T^{\text{tx}} \gamma_T F(r_{T,i})^{-2}} > \tau_T\right). \end{aligned} \quad (23)$$

Taking $S(r_{T,0}) = (1 + \tau_T) P_T^{\text{tx}} \gamma_T(r_{T,0})^{-2} \exp(-K_a r_{T,0}) - P_T^{\text{tx}} \gamma_T(r_{T,0})^{-2} \tau_T$, where, $I_T^{\text{agg}} = \sum_{i \in \Phi \setminus 0} P_T^{\text{tx}} \gamma_T F(r_{T,i})^{-2}$ is the cumulative interference at the typical mobile user and applying Gil-Pelaez inversion theorem, Eq. (23) can be rewritten as follows:

$$\begin{aligned} \mathbb{C}_T &= \mathbb{P}\left(\frac{S(r_{T,0})}{N_0 + I_T^{\text{agg}}} > \tau_T\right), \\ &= \mathbb{P}(S(r_{T,0}) > \tau_T N_0 + \tau_T I_T^{\text{agg}}), \\ &= \mathbb{E}_{r_{T,0}} \left[\frac{1}{2} - \frac{1}{\pi} \int_0^\infty \frac{\text{Im}[\phi_\Omega|_{r_{T,0}}(\omega) \exp(j\omega \tau_T N_0)]}{\omega} d\omega \right], \end{aligned} \quad (24)$$

where $\text{Im}(\cdot)$ denotes the imaginary operator, $\Omega = S(r_{T,0}) - \tau_T I_T^{\text{agg}}$, and $\phi_\Omega(\omega) = \mathbb{E}[\exp(-j\omega \Omega)]$ denotes the characteristic function (CF) of Ω can be stated as follows:

$$\phi_\Omega|_{r_{T,0}}(\omega) = \exp(-j\omega S(r_{T,0})) \mathcal{L}_{I_T^{\text{agg}}|_{r_{T,0}}}(-j\omega \tau_T). \quad (25)$$

where $\mathcal{L}_{I_T^{\text{agg}}|_{r_T}}$ is the LT of the cumulative interference conditioned on $r_{T,0}$ and is derived in the following Lemma.

Lemma 5. *The LT of the cumulative interference can be given as follows:*

$$\mathcal{L}_{I_T^{\text{agg}}}(s) = \exp\left(2\pi\lambda_T \sum_{l=1+\epsilon}^{\infty} \frac{(-sF\gamma_T P_T^{\text{tx}})^l}{(2l-2)!} \cdot \frac{1}{(r_{T,0})^{2l-2}}\right),$$

where $F = (\theta_{\text{tx}} \theta_{\text{rx}})/4\pi^2$ is the probability of main-lobe alignment of the interferers and the typical user and given negligible side lobe gains.

Proof. Starting from the definition of LT, we have:

$$\begin{aligned} \mathcal{L}_{I_T^{\text{agg}}}(s) &= \mathbb{E}_{\Phi_T} [\exp(-sI_T^{\text{agg}})] \\ &= \mathbb{E}_{\Phi_T} \left[\exp\left(-sF \sum_{i \in \Phi_T \setminus 0} P_T^{\text{tx}} \gamma_T(r_{T,i})^{-2}\right) \right], \\ &= \mathbb{E}_{\Phi_T} \left[\prod_{i \in \Phi_T \setminus 0} \exp\left(-sF P_T^{\text{tx}} \gamma_T(r_{T,i})^{-2}\right) \right], \\ &\stackrel{(a)}{=} \exp\left(-2\pi\lambda_T \int_{r_{T,0}}^{\infty} r_{T,i} \left(1 - \exp(-sF\gamma_T P_T^{\text{tx}}(r_{T,i})^{-2})\right) dr_{T,i}\right), \\ &\stackrel{(b)}{=} \exp\left(2\pi\lambda_T \int_{r_{T,0}}^{\infty} \sum_{l=1+\epsilon}^{\infty} \frac{(-sF\gamma_T P_T^{\text{tx}})^l}{(r_{T,i})^{2l-1} l!} dr_{T,i}\right), \\ &\stackrel{(c)}{=} \exp\left(2\pi\lambda_T \sum_{l=1+\epsilon}^{\infty} \frac{(-sF\gamma_T P_T^{\text{tx}})^l}{(2l-2)!} \frac{1}{(r_{T,0})^{2l-2}}\right), \end{aligned}$$

where using probability generating functional (**PGFL**) $f(x) = \exp(-sP_T h(r_{T,i}))$ step (a) has obtained, (b) is obtained by using $\exp(-x) = \sum_{i=0}^{\infty} (-1)^i \frac{x^i}{i!}$ ([37], Eq. 1.211) and $\epsilon = 0.01$ is inserted to avoid the indeterminate term. Since the mobile user has maintained a distance $r_{T,0}$ from its tagged TBS, all interferers are beyond $r_{T,0}$, which is the lower limit of the integral. ■

B. Conditional Coverage Probability - RF

The conditional probability of coverage of the mobile user, which is tagged to RBS can be derived in an interference limited regime as follows [9]:

$$\begin{aligned} \mathbb{C}_R &= \mathbb{P}\left(\frac{P_R^{\text{tx}} \gamma_R H}{(r_{R,0})^\alpha I_R^{\text{agg}}} > \tau_R\right) \\ &= \mathbb{P}(H > \tau_R (P_R^{\text{tx}})^{-1} \gamma_R^{-1} (r_{R,0})^\alpha I_R^{\text{agg}}), \\ &= \mathbb{E}[\exp(-\tau_R (P_R^{\text{tx}})^{-1} \gamma_R^{-1} (r_{R,0})^\alpha I_R^{\text{agg}})], \\ &= \int_0^\infty \mathcal{L}_{I_R^{\text{agg}}}(\tau_R (P_R^{\text{tx}})^{-1} \gamma_R^{-1} (r_{R,0})^\alpha) f_{r_{R,0}}(r_{R,0}) dr_{R,0}, \end{aligned} \quad (26)$$

where $\mathcal{L}_{I_R^{\text{agg}}}(\tau_R (P_R^{\text{tx}})^{-1} \gamma_R^{-1} (r_{R,0})^\alpha) = \exp(-\pi(r_{R,0})^2 \lambda_R \mathcal{Y}(\tau_R, \alpha))$. Here, $\mathcal{Y}(\tau_R, \alpha) = \frac{2\tau_R}{\alpha-2} {}_2F_1[1, 1 - \frac{2}{\alpha}; 2 - \frac{2}{\alpha}; -\tau_R]$, and ${}_2F_1[\cdot]$ is the Gauss's Hypergeometric function.

C. Coverage Probability With and Without Mobility

The overall coverage probability without mobility in a hybrid RF-THz network is given by substituting the conditional coverage probability results given in (30) and (26) into (22). The overall coverage probability with mobility is a function of HO probability. The coverage degrades with the higher HO probability, service delays, and dropped calls. The overall coverage with mobility can then be modeled as follows [12]:

$$\mathbb{C}_M = \mathbb{C}(1 - \eta \mathbb{P}(H)), \quad (27)$$

The coefficient η , in effect, measures the system sensitivity to HOs. Its value depends on a number of factors, e.g., the radio access technology, the mobility protocol, the protocol's layer

of operation and the link speed. At one extreme, as $\eta \rightarrow 0$, there is no HO cost and system HO failures do not happen. On the other hand, as $\eta \rightarrow 1$, every HO results in an outage. Note that \mathbb{C} is the total coverage probability of a typical mobile user in a hybrid RF-THz network without mobility given by (22) and $\mathbb{P}(H)$ is the overall HO probability for that mobile user in a hybrid RF-THz network given by (21).

Remark: As a special case, the overall coverage probability without mobility in a stand-alone THz network can be given simply by averaging (30) over d_0 instead of $r_{T,0}$.

Furthermore, in the case of noise-limited regime, i.e., when the interference is negligible, the coverage probability in a stand-alone THz network can be simplified as shown in the following.

Corollary 4. *In the noise-limited regime (in scenarios where the intensity of TBSSs is low), the coverage probability of a typical user can be simplified as follows:*

$$\begin{aligned} \mathbb{C}_T &= \mathbb{P}(S(r_{T,0}) > \tau_T N_0), \\ &\stackrel{(a)}{=} \mathbb{E}_{r_{T,0}} \left[\frac{1}{2} - \frac{1}{\pi} \int_0^\infty \frac{\text{Im}[\exp(-j\omega(S(r_{T,0}) - \tau_T N_0))]}{\omega} d\omega \right], \\ &= \frac{1}{2} + \frac{1}{\pi} \mathbb{E}_{r_{T,0}} \left[\int_0^\infty \frac{\sin(\omega(S(r_{T,0}) - \tau_T N_0))}{\omega} d\omega \right], \end{aligned} \quad (28)$$

where (a) follows from Euler's identity, i.e., $e^{-j\theta} = \cos\theta - j\sin\theta$.

D. Extension to Incorporate Misalignment

The misalignment errors in the desired signal can be incorporated with the path-loss as a normal random variable [38] with zero mean and finite variance. Let the LT of misalignment variable χ is given by $\mathcal{L}_\chi(\cdot)$, we can update the coverage probability calculation as follows:

$$\begin{aligned} \mathbb{C}_T &= \mathbb{P}\left(\frac{S(r_{T,0})\chi}{N_0 + I_T^{\text{agg}}} > \tau_T\right) = \mathbb{P}(S(r_{T,0})\chi > \tau_T N_0 + \tau_T I_T^{\text{agg}}), \\ &= \mathbb{E}_{r_{T,0}} \left[\frac{1}{2} - \frac{1}{\pi} \int_0^\infty \frac{\text{Im}[\phi_{\Omega|r_{T,0}}(\omega) \exp(j\omega\tau_T N_0)]}{\omega} d\omega \right], \end{aligned} \quad (29)$$

where $\Omega = S(r_{T,0})\chi - \tau_T I_T^{\text{agg}}$ and $\phi_{\Omega|r_{T,0}}(\omega) = \mathcal{L}_\chi(j\omega S(r_{T,0}))\mathcal{L}_{I_T^{\text{agg}}|r_{T,0}}(-j\omega\tau_T)$.

E. Extension to Incorporate Blockages

Along the lines of [32], the blockages can be modeled as a thinning process in the stochastic geometry models where the transmissions from a specific number of BSs are considered as blocked. Similar to [32], we consider a Boolean blockage model in which obstacles are rectangles and are distributed following a homogeneous PPP of density λ_B . The rectangles length (L_k) and width (W_k) are independent and identically distributed, and their probability density functions are $f_L(x)$ and $f_W(x)$, respectively. The orientation of these rectangles is distributed uniformly in $[0, 2\pi)$. Then, according to [32], the number of blockages in a link of length $r_{T,0}$ is a random variable with Poisson distribution having mean $\xi r_{T,0} + p$, where $\xi = \frac{2\lambda_B(E\{W\} + E\{L\})}{\pi}$ and $p = \lambda_B E\{W\} E\{L\}$, where

$0 < p < 1$ represents the area which is under blockages. Thus, the LOS probability is $p_{\text{LOS}}(r_{T,0}) = \exp[-(\xi r_{T,0} + p)]$ and this factor can be multiplied with the coverage probability to consider the impact of blockages. Subsequently, the coverage probability \mathbb{C}_T now depends on two events, i.e, (i) the LOS link is not blocked; and (ii) SINR_T is greater than τ_T . For a given distance $r_{T,0}$, \mathbb{C}_T can be expressed as in (30), where $\Omega = S(r_{T,0}) - \tau_T I_{\text{agg}}^T$.

F. Extension to Incorporate Ping-Pong Effect

Typically, in wireless networks, the handover is initiated if the received signal power of another BS becomes better than the current serving BS by at least by a predefined factor. To consider the ping-pong effect, we can incorporate a constant bias (hysteresis factor) η_H , i.e., by scaling the received signal power of the serving BS (whether RF or THz BS) in Section-II.C in a straight-forward manner. For higher values of η_H , the handoff probability (and thus ping-pong effect) will reduce. However, optimizing this factor is beyond the scope of this article and is an interesting future research direction.

V. NUMERICAL RESULTS AND DISCUSSIONS

In this section, the derived expressions has been validated by Monte-Carlo simulations with the consideration of a hybrid RF-THz network. Our results extract useful insights related to the probability of coverage of a moving user within a hybrid RF-THz network considering the impact of molecular noise in THz transmission, intensity of TBSSs, desired rate requirement, and velocity of a user. We have a general mobility model where the typical user can have any arbitrary trajectory with random distances and directions at each movement step.

A. Simulation Parameters

Unless stated otherwise, the users and BSs are located within a radius of 500 m circular region. The transmit power from TBS is 0.2 W and intensity of TBS is 0.0001 BSs/m². The transmit and receive antenna gains (i.e., G_T^{tx} and G_T^{rx}) of TBSSs are considered as 25 dB. Desired target rate is 1 Gbps and THz transmission bandwidth is taken as 0.5 GHz. On the other hand, the transmit power from RBS is 2 W, where its transmission frequency is 2 GHz and transmission bandwidth is 40 MHz. Here, the exponent of path loss α is 4, and the intensity of RBSs is 0.00001 BSs/m². First three terms of Lemma 5 provide a good approximation and are used to compute numerical results. The simulation parameters to compute $K_a(f)$ are listed in Table II.

B. Results and Discussions

Fig. 3(a) depicts the HO probability calculated for a typical mobile user who is tagged to TBS as a function of its velocity and intensity of the RBSs and TBSSs. We compare the accuracy of our numerical results with the corresponding simulation results and note that our analytical results match perfectly with the Monte-Carlo simulations. The molecular absorption coefficient is set as $K_a = 0.01\text{m}^{-1}$. We observe that the

$$\begin{aligned} \mathbb{C}_T &= p_{\text{LOS}}(r_{T,0}) \mathbb{P} \left(\frac{S(r_{T,0})}{N_0 + I_T^{\text{agg}}} > \tau_T \right), \\ &= \mathbb{E}_{r_{T,0}} \left[\frac{p_{\text{LOS}}(r_{T,0})}{2} - \frac{1}{\pi} \int_0^\infty p_{\text{LOS}}(r_{T,0}) \frac{\text{Im}[\phi_{\Omega|r_{T,0}}(\omega) \exp(j\omega\tau_T N_0)]}{\omega} d\omega \right], \end{aligned} \quad (30)$$

Table II
SIMULATION PARAMETERS FOR CALCULATING $K_a(f)$ [29]

Symbol	Value	Symbol	Value
p_0, p	1 atm, 1 atm	$q^{(i,g)}$	0.05 [%]
T_0, T	296 K, 396 K	k_b	1.3806×10^{-23} J/K
$f_{e_0}^{(i,g)}$	276 Hz	T_{sp}	273.15 K
γ	0.83	N_A	6.0221×10^{23}
$S^{(i,g)}$	2.66×10^{-25} Hz-m ² /mol	h	6.6262×10^{-34} J s
$\alpha_0^{(i,g)}, \alpha_{\text{air}}^{(i,g)}$	0.916Hz, 0.1117Hz	c	2.9979×10^8 m/s
$\delta^{(i,g)}$	0.0251 Hz	V	8.2051×10^{-5} m ³ atm/K/mol

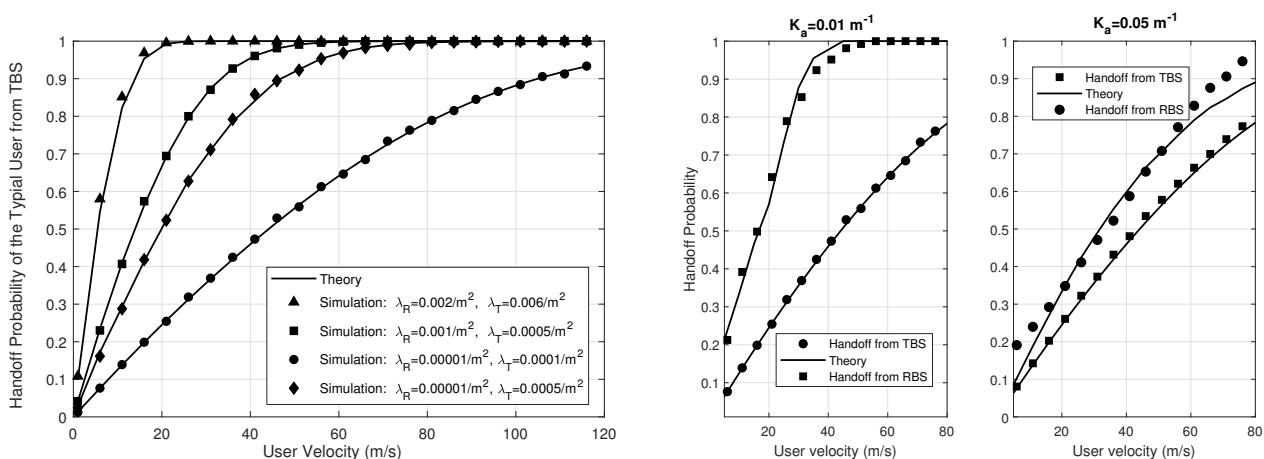


Figure 3. (a) HO probability of a typical user from TBS as a function of the velocity and intensity of TBSs, $K_a = 0.01 \text{ m}^{-1}$. (b) HO probability of a typical user as a function of the velocity and molecular absorption in a hybrid RF-THz network, $\lambda_R = 0.00001$ per m^2 and $\lambda_T = 0.0001$ per m^2 .

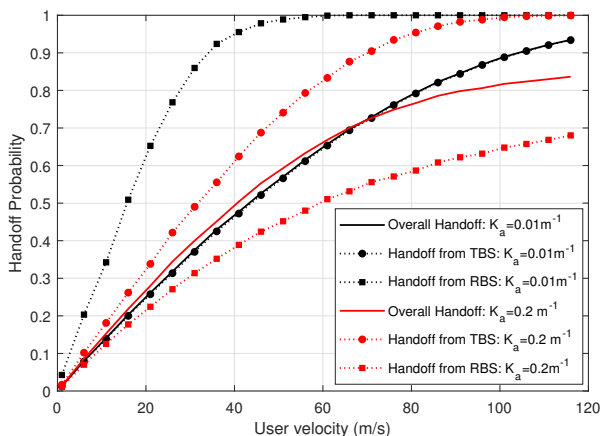


Figure 4. Overall HO probability of a typical user as a function of the velocity and molecular absorption in a hybrid RF-THz network, $\lambda_R = 0.00001$ per m^2 and $\lambda_T = 0.0001$ per m^2 .

HO probability increases with the increase in the number of RBSs; however, the increase is much more significant with the increase in TBSs. That is, we note that increasing λ_T from 0.0001 to 0.0005 per m^2 [i.e., almost 5 times] at $\lambda_R = 0.00001$ per m^2 increases the HO probability much more compared to the case when λ_R increases from 0.00001 to 0.001 per m^2 [i.e., almost 100 times] at $\lambda_T = 0.0005$ per m^2 . This signifies the impact of severe molecular absorption and small coverage zones on the connectivity of mobile users transmitting in a hybrid RF-THz network.

Fig. 3(b) depicts the impact of user's velocity on the conditional HO probability from TBS and conditional HO probability from RBS considering two different absorption coefficients, i.e., $K_a = 0.01 \text{ m}^{-1}$ and $K_a = 0.05 \text{ m}^{-1}$. For lower values of K_a , the HO probability is much higher if the user was initially associated to RBS compared to the case if the user was initially connected to TBS. Also, in this case, the HO probability increases much rapidly with the increase in velocity. The reason is the high-received signal power from TBS compared to RBS generates more BS-switching. Conversely, for higher molecular absorption (i.e., $K_a = 0.05$

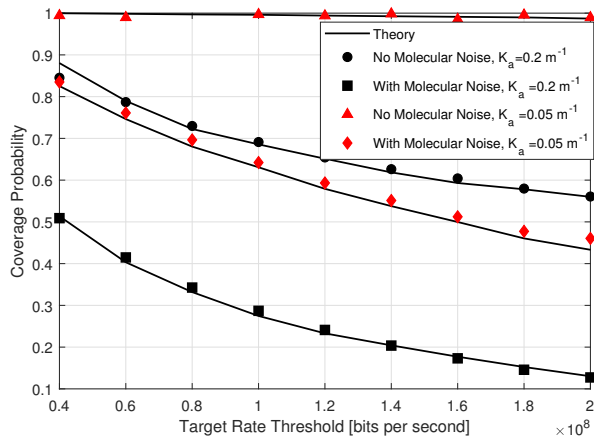


Figure 5. Coverage probability of a typical user as a function of the target rate threshold (in bps, $\lambda_R = 0.00001$ per m^2 and $\lambda_T = 0.0001$ per m^2).

m^{-1}), we note an opposite trend. That is, the HO probability is much higher if the user was initially associated to TBS compared to the case when the user was initially connected to RBS. The reason is the severe molecular absorption which degrades the received signal from TBS and favors shifting users from TBS to RBS. Finally, it can be observed that as the molecular absorption coefficient $K_a \rightarrow 0$, our analytical results matches perfectly with the Monte-Carlo simulations. Conversely, for $K_a = 0.05$, the impact of approximation can be observed clearly. Note that the HO from TBS is exact and the approximation is only in the HO from RBS.

Fig. 4 has been plotted by keeping the intensity of BSs fixed (i.e., $\lambda_R = 0.00001$ per m^2 and $\lambda_T = 0.0001$ per m^2) and tracking the variation of the HO probability from TBS (H_T), HO probability from RBS (H_R), and overall HO probability of a typical mobile user with different molecular absorption coefficients. In the figure, the black curves consider $K_a = 0.01 m^{-1}$, whereas the red curves assume $K_a = 0.2 m^{-1}$. It can be observed that for low molecular absorption coefficient, the HO probability from RBS is much higher. The reason is that the lower molecular absorption favours association with TBS due to higher received powers. Conversely, when the molecular absorption coefficient is high, the HO probability from TBS is much higher, i.e., for the user who is initially associated with TBS. The reason is that the impact of molecular absorption is devastating; therefore, the criterion favours association with RBS. Nevertheless, the overall HO probability remains nearly the same which highlights the significance of computing and extracting insights from (H_T) and (H_R) separately.

Fig. 5 demonstrates the impact of thermal and molecular absorption noise on the coverage probability of a static user for two different molecular absorption coefficients, K_a , as a function of user's desired data rate. Our analytical results match well with the simulation results. As expected, the coverage probability decreases with the increase in the target data rate. Furthermore, the impact of molecular noise is devastating and substantiate that ignoring molecular noise from the analytical

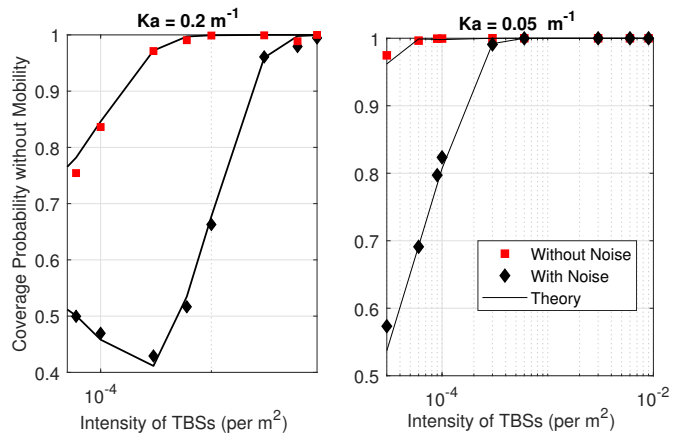


Figure 6. Coverage probability of a typical user as a function of the intensity of TBSs and molecular absorption in a hybrid RF-THz network, $K_a = 0.05m^{-1}$ and $K_a = 0.01m^{-1}$.

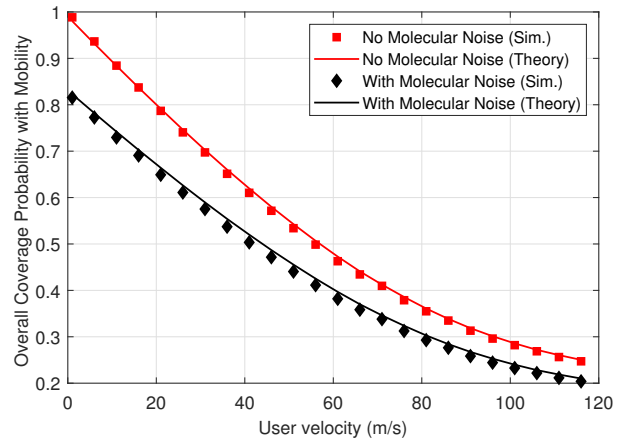


Figure 7. Mobility-aware coverage probability with a relation of a function of the user's velocity with and without molecular absorption, $\mu = 0.82$, $K_a = 0.05m^{-1}$.

results (as is done in [9]) can lead to over-optimistic results. Furthermore, with the increase in molecular absorption, the coverage probability degrades considerably.

Fig. 6 depicts the coverage probability with and without molecular noise as a function of the intensity of TBSs. The intensity of RBSs kept constant, and the user is static, however, the coverage probability is observed for two different values of molecular absorption coefficient. The analytical results corroborate with the simulation results. This figure also confirms that the molecular noise significantly degrades the coverage probability compared to the case when there is no molecular noise [9]. Furthermore, in general, the increase in intensity of TBSs increases coverage due to the shortening of distance from the nearest TBS. Interestingly, when molecular absorption is high, increasing the intensity first deteriorates the coverage probability (due to increased interference); and afterwards escalate due to improved signal quality which is

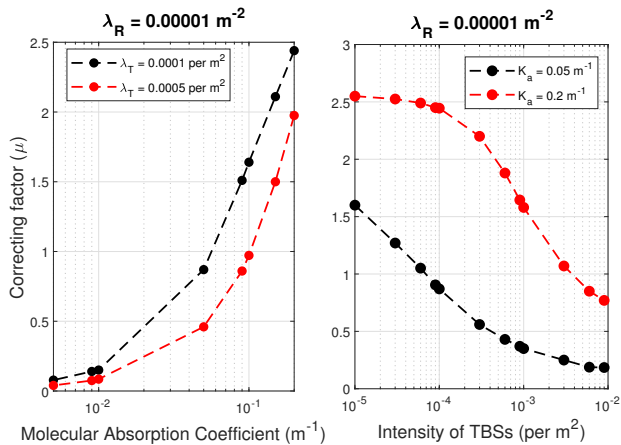


Figure 8. The correction factor as a function of the intensity of the TBSs and molecular absorption.

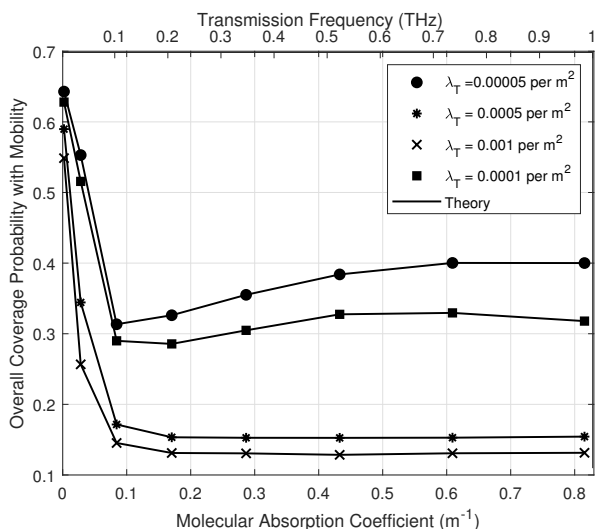


Figure 9. Overall coverage probability of a typical user with mobility as a function of the molecular absorption coefficients and frequencies considering molecular noise and a constant user's velocity.

mainly due to shorter distance from the associated TBS.

Fig. 7, demonstrate the overall coverage probability with mobility from Eq. (27) as a function of user's velocity. Numerical values from simulation results validate the accuracy of our theoretical results. This figure confirms the overall coverage probability reduces with the increase in velocity and demonstrates the gap between the results with molecular noise and without molecular noise in [9].

Fig. 8 illustrates the correcting factor (μ) as a function of the molecular absorption coefficient (K_a) and intensity of TBSs considering a fixed intensity of RBSs. The figure shows that the correcting factor gradually increases with the increasing value of molecular absorption coefficient. On the other hand, the figure demonstrates that the correcting factor gradually decreases with the increasing intensities of TBSs.

Fig. 9 depicts the overall coverage probability with mobility

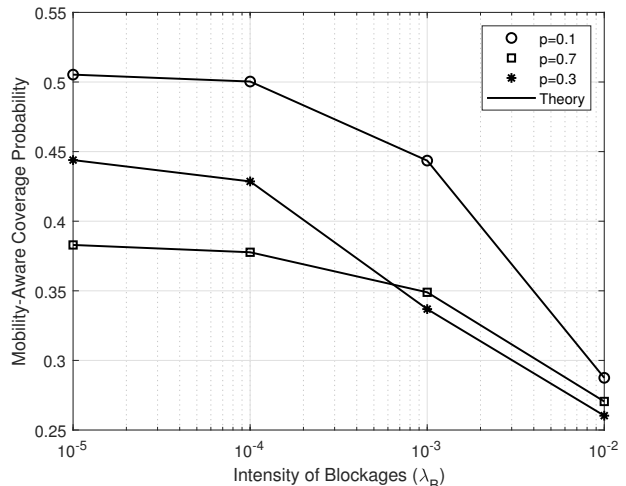


Figure 10. Overall coverage probability of a typical user with mobility as a function of the intensity of blockages.

as a function of the molecular absorption coefficient and intensity of TBSs. We consider the user is moving with a constant velocity (i.e., 56 m/s). The higher intensity of TBSs ($\lambda_T = 0.001$ per m^2 and $\lambda_T = 0.0005$ per m^2) results in a much denser THz network and the connected TBSs are likely to be much closer to the moving user. Therefore, increasing value of molecular absorption simply degrades the probability of coverage. This degradation is due to the reduction in signal strength. However, a more interesting observation can be noted from the cases when $\lambda_T = 0.0001$ per m^2 and $\lambda_T = 0.00005$ per m^2 . That is, the overall coverage probability first reduces due to the signal degradation as a function of the molecular absorption. However, the coverage starts increasing again at some point and the reason is the reduction in interference with the increase of molecular absorption coefficient. Surprisingly, the benefits of interference reduction due to increasing molecular absorption dominates the drawback of signal degradation for a reasonable intensity of TBSs. This trend is opposite to what observed for much denser THz network.

Finally, Fig. 10 denotes the impact of blockage intensity λ_B or blockage area p on the coverage probability. As expected, increasing either λ_B or p results in the coverage degradation.

VI. CONCLUSIONS AND FUTURE WORK

In this article, we provided a comprehensive stochastic geometry framework to describe the overall performance of a mobile user in a two-tier hybrid RF-THz network. We derived novel coverage probability expressions considering molecular noise in THz transmissions and derived the coverage probability with mobility. We validated the accuracy of derived expressions using Monte-Carlo simulations. Our numerical results depict that the probability of HO in THz network is of much more significance than in conventional RF network, especially for lower molecular absorption coefficients. Therefore, mobility-aware performance frameworks are of immediate relevance. Also, our results demonstrated

that the benefits of interference reduction due to increasing molecular absorption can dominate compared to the signal degradation at reasonable intensity of TBSs. This is favourable news for upcoming 6G networks. Furthermore, our results revealed that ignoring molecular absorption and mobility can lead to significantly over-optimistic results, especially in high frequency THz networks. In this paper, we considered the standard procedure of performing handoff based on the received signal power measurements from different access points. However, developing sophisticated handoff mechanisms for short-range transmissions is an interesting research topic for further investigation. Furthermore, to capture the distinct coverage zones, transmit powers, deployment intensity, and channel propagation, we consider complementing THz with RF. However, the proposed framework can be extended for mm-wave based model by modifying the path-loss model of RF or THz, as needed.

APPENDIX A PROOF OF LEMMA 1

Given the event $k = T$ is defined as the event when user is associated to TBS, then the conditional PDF of the distance from the connected TBS can be obtained as follows:

$$f_{r_T}(r_T) = \frac{1}{A_T} \frac{d\mathbb{P}(d_0 > r_T, k = T)}{dd_0}. \quad (\text{A.1})$$

Subsequently, the joint PDF in the numerator can be derived as follows:

$$\begin{aligned} \mathbb{P}(d_0 > r_T, k = T) &= \mathbb{P}(d_0 > r_T, P_T^{\text{rx}} > P_R^{\text{rx}}), \\ &= \int_{r_T}^{\infty} \mathbb{P}(P_T^{\text{rx}} > P_R^{\text{rx}}) f_{d_0}(d_0) dd_0, \\ &= \int_{r_T}^{\infty} \mathbb{P}\left(P_T \gamma_T \frac{\exp(-K_a d_0)}{d_0^2} > P_R \gamma_R r_0^{-\alpha}\right) f_{d_0}(d_0) dd_0, \\ &\stackrel{(a)}{=} \int_{r_T}^{\infty} 2\pi \lambda_T d_0 e^{(-\pi \lambda_T d_0^2 - \pi \lambda_R (d_0^2 Q)^{\frac{2}{\alpha}} \exp(\frac{2K_a d_0}{\alpha}))} dd_0, \end{aligned} \quad (\text{A.2})$$

where (a) follows from substituting $\mathbb{P}(P_T^{\text{rx}} > P_R^{\text{rx}})$ in (18), and $f_{d_0}(d_0) = 2\pi \lambda_T d_0 \exp(-\pi \lambda_T d_0^2)$. Now the final value of $f_{r_T}(r_T)$ is obtained by replacing (A.2) into (A.1). Similarly, the event $k = R$ is defined as the event when user is associated to RBS, then the conditional PDF of the distance from the tagged RBS can be derived as follows:

$$f_{r_R}(r_R) = \frac{1}{A_R} \frac{d\mathbb{P}(r_0 > r_R, k = R)}{dr_R}. \quad (\text{A.3})$$

Subsequently, the joint PDF in the numerator of (A.3) can be derived as follows:

$$\begin{aligned} \mathbb{P}(r_0 > r_R, k = R) &= \mathbb{P}(r_0 > r_R, P_R^{\text{rx}} > P_T^{\text{rx}}), \\ &= \int_{r_R}^{\infty} \mathbb{P}(P_R^{\text{rx}} > P_T^{\text{rx}}) f_{r_0}(r_0) dr_0, \\ &= \int_{r_R}^{\infty} \mathbb{P}\left(P_R \gamma_R r_0^{-\alpha} > P_T \gamma_T \frac{\exp(-K_a d_0)}{d_0^2}\right) f_{r_0}(r_0) dr_0, \\ &\stackrel{(a)}{\approx} \int_{r_R}^{\infty} \mathbb{P}\left(P_R \gamma_R r_0^{-\alpha} > P_T \gamma_T d_0^{2-\mu}\right) f_{r_0}(r_0) dr_0, \\ &= \int_{r_R}^{\infty} 2\pi \lambda_R r_0 \exp\left(-\pi \lambda_R r_0^2 - \pi \lambda_T \left(\frac{r_0^\alpha}{Q}\right)^{\frac{2}{2+\mu}}\right) dr_0, \end{aligned} \quad (\text{A.4})$$

where the approximation $r_T^2 \exp(K_a r_T)$ with $r^{2+\mu}$ and the efficient choice of correcting factor μ (as discussed in Section III) help to derive the expression in step (a). Finally, substituting (A.4) in (A.1) yields $f_{r_T}(r_T)$ as given in **Lemma 1**. Here, $f_{r_0}(r_0) = 2\pi \lambda_R r_0 \exp(-\pi \lambda_R r_0^2)$ and $f_{d_0}(d_0) = 2\pi \lambda_T d_0 \exp(-\pi \lambda_T d_0^2)$.

APPENDIX B PROOF OF LEMMA 2

It can be observed from Fig. 2(a) that the vertical HO between RF and THz tiers does not occur if all BSs within these two tiers except tagged BS (i.e., TBS) are situated outside the area $|B' \setminus B' \cap A'|$. When the distance is r_T and the direction (or angle) of user movement is θ , there will be no HO from the serving TBS with probability as follows:

$$\begin{aligned} \mathbb{P}(\bar{H}_T | r_T, \theta) &= \mathbb{P}(N(|B' \setminus B' \cap A'|) = 0 | T_T \neq T_R) \\ &\quad + \mathbb{P}(N(|B \setminus B \cap A|) = 0 | T_T = T_R), \end{aligned} \quad (\text{B.1})$$

where \bar{H}_T is the complement of H_T and $N(\cdot)$ presents the number of BSs within a particular area. Here, T_T and T_R simplifies the THz and RF tier, respectively. After averaging over r_T and θ , $\mathbb{P}[H_T]$ is given in **Lemma 2**. The first expression in Eq. (B.1) states the vertical HO and the second expression is the horizontal HO. Finally, applying the null property of the PPP, we have:

$$\mathbb{P}(\bar{H}_T | r_T, \theta) = e^{\lambda_T |B \setminus B \cap A| + \lambda_R |B' \setminus B' \cap A'|}. \quad (\text{B.2})$$

Here, $B = \pi R_T^2$, $B' = \pi R_R^2$. From Fig. 11, the part of expression in Eq. (B.2), $|B \cap A|$ can be easily determined as follows:

$$\begin{aligned} |B \cap A| &= R_T^2 \cos^{-1}\left(\frac{R_T^2 + v^2 - r_T^2}{2R_T^2 v}\right) + r_T^2 \cos^{-1}\left(\frac{r_T^2 + v^2 - R_T^2}{2r_T^2 v}\right) \\ &\quad - \frac{1}{2} \sqrt{(r_T + R_T - v)(r_T + R_T + v)(v + r_T - R_T)(v - r_T + R_T)}, \\ &= R_T^2 \theta_1^T + r_T^2 (\pi - \theta) - r_T v \sin \theta. \end{aligned} \quad (\text{B.3})$$

Similarly, the term $|B' \cap A'|$ can also be calculated from Fig. 11 as follows:

$$\begin{aligned} |B' \cap A'| &= R_R'^2 \cos^{-1}\left(\frac{R_R'^2 + v^2 - r_R'^2}{2R_R'^2 v}\right) + r_R'^2 \theta_2^T \\ &\quad - \frac{1}{2} \sqrt{(r_R' + R_R' - v)(r_R' + R_R' + v)(v + r_R' - R_R')(v - r_R' + R_R')}, \\ &= R_R'^2 \theta_3^T + r_R'^2 (\pi - \theta_2^T) - r_R' v \sin \theta_2^T. \end{aligned} \quad (\text{B.4})$$

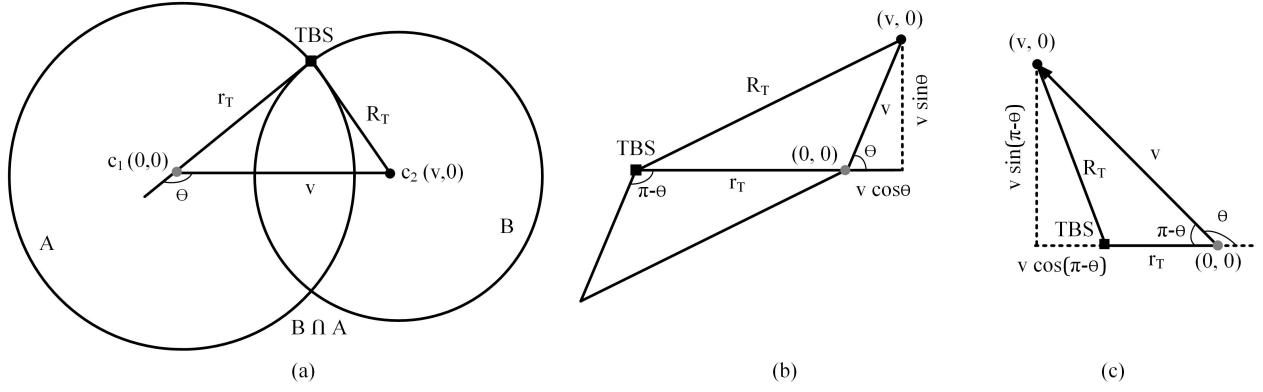


Figure 11. (a) Geometrical illustration of r_T , R_T , v and θ , (b) $0 \leq \theta < \frac{\pi}{2}$, (c) $\frac{\pi}{2} \leq \theta \leq \pi$.

The common area between two intersecting tiers can be calculated from Eq. (B.3) and Eq. (B.4), where $R_T^2 = r_T^2 + v^2 - 2r_T v \cos(\pi - \theta)$, $R'_R = (R_T)^\alpha e^{\frac{K_a R_T}{\alpha}} \left(\frac{P_R^{tx} Q}{P_T^{tx}} \right)^{\frac{1}{\alpha}}$, $r'_R = (r_T)^\alpha e^{\frac{K_a R_T}{\alpha}} \left(\frac{P_R^{tx} Q}{P_T^{tx}} \right)^{\frac{1}{\alpha}}$, $\theta_1^T = \theta - \sin^{-1} \left(\frac{v \sin \theta}{R_T} \right)$, $\theta_2^T = \cos^{-1} \left(\frac{r_R^2 + v^2 - R_R^2}{2r'_R v} \right)$, $\theta_3^T = \theta - \sin^{-1} \left(\frac{v \sin \theta}{R'_R} \right)$.

According to the Fig. 2(a), the common area between two intersecting circles of radii r_T and R_T is S_T . Here, the value of $\theta_1^T = \theta - \sin^{-1} \left(\frac{v \sin \theta}{R_T} \right)$, which is true when the value of θ lies between 0 and $\frac{\pi}{2}$. According to Fig. 11(c), when the value of θ is in between $\frac{\pi}{2}$ and π then r is no longer greater than $\{v \cos(\pi - \theta)\}$ or in other words, $v \cos(\pi - \theta) > r$. For $\frac{\pi}{2} \leq \theta \leq \pi$ from [39], $\left\{ \sin^{-1} \left(\frac{v \sin \theta}{R_T} \right) \right\}$ in θ_1^T will be replaced by $\left\{ \pi - \sin^{-1} \left(\frac{v \sin \theta}{R_T} \right) \right\}$. Therefore, we define a new term C_T with modified θ_1^T to substitute the term S_T in **Lemma 2**.

On the contrary, the common area between two intersecting circles from radii r'_R and R'_R is S'_T . For $\frac{\pi}{2} \leq \theta_2^T \leq \pi$ from [39], $\left\{ \sin^{-1} \left(\frac{v \sin \theta_2^T}{R'_R} \right) \right\}$ in θ_3^T will be replaced by $\left\{ \pi - \sin^{-1} \left(\frac{v \sin \theta_2^T}{R'_R} \right) \right\}$. Therefore, we define a new term C'_T with modified θ_3^T to substitute the term S'_T in **Lemma 2**.

APPENDIX C PROOF OF LEMMA 4

The vertical HO between THz and RF tiers does not occur if all BSs except tagged RBSs are located outside the area $|A' \setminus A' \cap B'|$. When the distance is r_R and the direction (or angle) of the user movement is θ , there will be no HO from the serving RBS with probability as follows:

$$\mathbb{P}(\overline{H}_R | r_R, \theta) = \mathbb{P}(N(|A' \setminus A' \cap B'|) = 0 | T_R \neq T_T) \quad (\text{C.1})$$

$$+ \mathbb{P}(N(|A \setminus A \cap B|) = 0 | T_R = T_T), \quad (\text{C.2})$$

where \overline{H}_R is the complement of H_R and $N(\cdot)$ depicts the number of BSs within a particular area. The first expression in Eq. (C.1) states the vertical HO and the second expression determines the horizontal HO. Finally, applying the null property of the PPP, we have:

$$\mathbb{P}(\overline{H}_R | r_R, \theta) = \exp(\lambda_R \cdot |A \setminus A \cap B| + \lambda_T \cdot |A' \setminus A' \cap B'|). \quad (\text{C.3})$$

Here, $A = \pi R_R^2$, $A' = \pi R_T'^2$. Likewise appendix B, it can be determined the two-parts of Eq. (C.3), i.e., $|A \cap B|$ and $|A' \cap B'|$ can be given as in the following:

$$\begin{aligned} |A \cap B| &= R_R^2 \cos^{-1} \left(\frac{R_R^2 + v^2 - r_T^2}{2R_R^2 v} \right) + r_T^2 \cos^{-1} \left(\frac{r_T^2 + v^2 - R_R^2}{2r_T^2 v} \right) \\ &\quad - \frac{1}{2} \sqrt{(r_R + R_R - v)(r_R + R_R + v)(v + r_R - R_R)(v - r_R + R_R)}, \\ &= R_R^2 \theta_1^R + r_T^2 (\pi - \theta) - r_R v \sin \theta. \end{aligned} \quad (\text{C.4})$$

$$\begin{aligned} |A' \cap B'| &= R_T'^2 \cos^{-1} \left(\frac{R_T'^2 + v^2 - r_T'^2}{2R_T'^2 v} \right) + r_T'^2 \theta_2^R \\ &\quad - \frac{1}{2} \sqrt{(r'_T + R'_T - v)(r'_T + R'_T + v)(v + r'_T - R'_T)(v - r'_T + R'_T)}, \\ &= R_T'^2 \theta_3^R + r_T'^2 (\pi - \theta_2^R) - r'_T v \sin \theta_2^R. \end{aligned} \quad (\text{C.5})$$

The common area between two intersecting tiers can be calculated from Eq. (C.4) and Eq. (C.5), where $R_R^2 = r_R^2 + v^2 - 2r_R v \cos(\pi - \theta)$, $R'_T = [(R_R)^\alpha \left(\frac{P_T^{tx} Q}{P_R^{tx}} \right)]^{\frac{1}{2+\mu}}$, $r'_T = [(r_R)^\alpha \left(\frac{P_T^{tx} Q}{P_R^{tx}} \right)]^{\frac{1}{2+\mu}}$, $\theta_1^R = \theta - \sin^{-1} \left(\frac{v \sin \theta}{R_R} \right)$, $\theta_2^R = \cos^{-1} \left(\frac{r_T'^2 + v^2 - R_T'^2}{2r_T' v} \right)$, $\theta_3^R = \theta - \sin^{-1} \left(\frac{v \sin \theta}{R'_R} \right)$.

According to the Fig. 1(b), the common area between two intersecting circle with radii r_R and R_R is S_R . Here, the value of $\theta_1^R = \theta - \sin^{-1} \left(\frac{v \sin \theta}{R_R} \right)$, which is true when the value of θ lies between 0 and $\frac{\pi}{2}$. Similar way as Fig. 11 (c), when $\frac{\pi}{2} \leq \theta \leq \pi$ then, $v \cos(\pi - \theta) > r$. For $\frac{\pi}{2} \leq \theta \leq \pi$ from [39], θ_1^R becomes $\left\{ \theta - \pi + \sin^{-1} \left(\frac{v \sin \theta}{R_R} \right) \right\}$. Therefore, a new term C_R is defined by modifying θ_1^R to substitute the term S_R in **Lemma 4**.

Likewise, the common area between two intersecting circles of radii r'_T and R'_T is S'_R , and later term C'_R with modified θ_3^R to substitute the term S'_R in **Lemma 4**.

REFERENCES

- [1] S. Mumtaz, J. M. Jornet, J. Aulin, W. H. Gerstacker, X. Dong, and B. Ai, "Terahertz communication for vehicular networks," *IEEE Trans. on Vehicular Technology*, vol. 66, no. 7, pp. 5617–5625, 2017.
- [2] N. Savage, "Autonomous cars drive terahertz research," <https://spie.org/news/photronics-focus/marapr-2021/autonomous-cars-drive-terahertz-research?SSO=1>, Mar. 2021.

- [3] J. Kokkonen, J. Lehtomäki, and M. Juntti, "Stochastic analysis of multi-tier nanonetworks in THz band," in *Proceedings of the 4th ACM Intl. Conf. on Nanoscale Computing and Commun.*, 2017, p. 30.
- [4] C. Chaccour, R. Amer, B. Zhou, and W. Saad, "On the reliability of wireless virtual reality at terahertz (THz) frequencies," in *2019 10th IFIP International Conference on New Technologies, Mobility and Security (NTMS)*, 2019, pp. 1–5.
- [5] X. Yao, C. Wang, and C. Qi, "Interference and coverage analysis for indoor THz communications with beamforming antennas," in *IEEE/CIC Intl. Conf. on Commun. Workshops in China (ICCC Workshops)*, 2019, pp. 147–152.
- [6] A. Shafie, N. Yang, and C. Han, "Multi-connectivity for indoor terahertz communication with self and dynamic blockage," in *IEEE Intl. Conf. on Commun. (ICC)*, 2020, pp. 1–7.
- [7] A. A. Boulogeorgos and A. Alexiou, "Error analysis of mixed THz-RF wireless systems," *IEEE Commun. Letters*, vol. 24, no. 2, pp. 277–281, 2020.
- [8] K. Ntontin and C. Verikoukis, "Toward the performance enhancement of microwave cellular networks through THz links," *IEEE Trans. on Vehicular Technology*, vol. 66, no. 7, pp. 5635–5646, 2016.
- [9] J. Sayehvand and H. Tabassum, "Interference and coverage analysis in coexisting RF and dense terahertz wireless networks," *IEEE Wireless Commun. Letters*, vol. 9, no. 10, pp. 1738–1742, 2020.
- [10] S. Sadr and R. S. Adve, "Handoff rate and coverage analysis in multi-tier heterogeneous networks," *IEEE Trans. on Wireless Commun.*, vol. 14, no. 5, pp. 2626–2638, 2015.
- [11] S.-Y. Hsueh and K.-H. Liu, "An equivalent analysis for handoff probability in heterogeneous cellular networks," *IEEE Commun. Letters*, vol. 21, no. 6, pp. 1405–1408, 2017.
- [12] C. Chen and X. Zhao, "Mobility-aware access strategy in multi-user hetnets," *IEEE Wireless Commun. Letters*, vol. 9, no. 7, pp. 1004–1008, 2020.
- [13] S. Choi, J.-G. Choi, and S. Bahk, "Mobility-aware analysis of millimeter wave communication systems with blockages," *IEEE Trans. on Vehicular Technology*, vol. 69, no. 6, pp. 5901–5912, 2020.
- [14] B. Yang, X. Yang, X. Ge, and Q. Li, "Coverage and handover analysis of ultra-dense millimeter-wave networks with control and user plane separation architecture," *IEEE Access*, vol. 6, pp. 54739–54750, 2018.
- [15] S. Nikhat and M. Mehmet-Ali, "A performance evaluation of millimeter-wave cellular networks with user mobility," in *IEEE Canadian Conference on Electrical & Computer Engineering (CCECE)*, 2018, pp. 1–6.
- [16] J. G. Andrews, T. Bai, M. N. Kulkarni, A. Alkhateeb, A. K. Gupta, and R. W. Heath, "Modeling and analyzing millimeter wave cellular systems," *IEEE Trans. on Commun.*, vol. 65, no. 1, pp. 403–430, 2016.
- [17] A. S. Cacciapuoti, R. Subramanian, K. R. Chowdhury, and M. Caleffi, "Software-defined network controlled switching between millimeter wave and terahertz small cells," *arXiv preprint arXiv:1702.02775*, 2017.
- [18] X. Lin, R. K. Ganti, P. J. Fleming, and J. G. Andrews, "Towards understanding the fundamentals of mobility in cellular networks," *IEEE Trans. on Wireless Commun.*, vol. 12, no. 4, pp. 1686–1698, 2013.
- [19] H. S. Dhillon, R. K. Ganti, and J. G. Andrews, "A tractable framework for coverage and outage in heterogeneous cellular networks," in *2011 Information Theory and Applications Workshop*. IEEE, 2011, pp. 1–6.
- [20] H. S. Dhillon, R. K. Ganti, F. Baccelli, and J. G. Andrews, "Modeling and analysis of K-tier downlink heterogeneous cellular networks," *IEEE Journal on Sel. Areas in Commun.*, vol. 30, no. 3, pp. 550–560, 2012.
- [21] H.-S. Jo, Y. J. Sang, P. Xia, and J. G. Andrews, "Heterogeneous cellular networks with flexible cell association: A comprehensive downlink SINR analysis," *IEEE Trans. on Wireless Commun.*, vol. 11, no. 10, pp. 3484–3495, 2012.
- [22] Q. Ye, B. Rong, Y. Chen, M. Al-Shalash, C. Caramanis, and J. G. Andrews, "User association for load balancing in heterogeneous cellular networks," *IEEE Trans. on Wireless Commun.*, vol. 12, no. 6, pp. 2706–2716, Jun. 2013.
- [23] J. Rubio, A. Pascual-Iserte, J. del Olmo, and J. Vidal, "User association strategies in HetNets leading to rate balancing under energy constraints," *EURASIP Journal on Wireless Commun. and Networking*, vol. 2017, no. 1, p. 204, 2017.
- [24] Q. Ye, O. Y. Bursalioglu, H. C. Papadopoulos, C. Caramanis, and J. G. Andrews, "User association and interference management in massive MIMO HetNets," *IEEE Trans. on Commun.*, vol. 64, no. 5, pp. 2049–2065, 2016.
- [25] A. Zappone, L. Sanguinetti, and M. Debbah, "User association and load balancing for massive MIMO through deep learning," in *52nd Asilomar Conf. on Signals, Systems, and Computers*. IEEE, 2018, pp. 1262–1266.
- [26] V. Petrov, M. Komarov, D. Moltchanov, J. M. Jornet, and Y. Koucheryavy, "Interference and SINR in millimeter wave and terahertz communication systems with blocking and directional antennas," *IEEE Trans. on Wireless Commun.*, vol. 16, no. 3, pp. 1791–1808, 2017.
- [27] J. Ma, R. Shrestha, L. Moeller, and D. M. Mittleman, "Invited article: Channel performance for indoor and outdoor terahertz wireless links," *APL Photonics*, vol. 3, no. 5, p. 051601, 2018.
- [28] J. F. Federici, J. Ma, and L. Moeller, "Review of weather impact on outdoor terahertz wireless communication links," *Nano Communication Networks*, vol. 10, pp. 13–26, 2016.
- [29] J. M. Jornet and I. F. Akyildiz, "Channel modeling and capacity analysis for electromagnetic wireless nanonetworks in the terahertz band," *IEEE Trans. on Wireless Commun.*, vol. 10, no. 10, pp. 3211–3221, 2011.
- [30] L. S. Rothman, I. E. Gordon, A. Barbe, D. C. Benner, P. F. Bernath, M. Birk, V. Boudon, L. R. Brown, A. Campargue, J.-P. Champion *et al.*, "The HITRAN 2008 molecular spectroscopic database," *Journal of Quantitative Spectroscopy and Radiative Transfer*, vol. 110, no. 9–10, pp. 533–572, 2009.
- [31] M. Di Renzo, "Stochastic geometry modeling and analysis of multi-tier millimeter wave cellular networks," *IEEE Trans. on Wireless Commun.*, vol. 14, no. 9, pp. 5038–5057, 2015.
- [32] T. Bai, R. Vaze, and R. W. Heath, "Analysis of blockage effects on urban cellular networks," *IEEE Trans. on Wireless Commun.*, vol. 13, no. 9, pp. 5070–5083, 2014.
- [33] V. Petrov, D. Moltchanov, and Y. Koucheryavy, "Interference and SINR in dense terahertz networks," in *IEEE 82nd Vehicular Technology Conference (VTC2015-Fall)*, 2015, pp. 1–5.
- [34] C. Chaccour and W. Saad, "On the ruin of age of information in augmented reality over wireless terahertz (THz) networks," in *GLOBECOM 2020 - 2020 IEEE Global Commun. Conference*, 2020, pp. 1–6.
- [35] P. Boronin, D. Moltchanov, and Y. Koucheryavy, "A molecular noise model for THz channels," in *2015 IEEE International Conference on Commun. (ICC)*, 2015, pp. 1286–1291.
- [36] J. Kokkonen, J. Lehtomäki, and M. Juntti, "A discussion on molecular absorption noise in the terahertz band," *Nano Communication Networks*, vol. 8, pp. 35–45, Jun. 2016.
- [37] I. S. Gradshteyn and I. M. Ryzhik, *Table of integrals, series, and products*. Academic press, 2014.
- [38] A. R. Ekti, A. Boyaci, A. Alparslan, İ. Ünal, S. Yarkan, A. Görçin, H. Arslan, and M. Uysal, "Statistical modeling of propagation channels for terahertz band," in *IEEE conf. on Standards for Commun. and Networking (CSCN)*, 2017, pp. 275–280.
- [39] H. Tabassum, M. Salehi, and E. Hossain, "Fundamentals of mobility-aware performance characterization of cellular networks: A tutorial," *IEEE Commun. Surveys & Tutorials*, vol. 21, no. 3, pp. 2288–2308, 2019.



Md. Tanvir Hossain Md Tanvir Hossain received his MASc degree in Electrical and Computer Engineering from York University, Canada in April 2021. He also received his MSc degree in Electronics Engineering from Kookmin University, South Korea, in 2018. His research interests include wireless communications including space communications, vehicular communications, and machine learning.



Hina Tabassum (SM'17) is currently an Assistant Professor at the Lassonde School of Engineering, York University, Canada. Prior to that, she was a postdoctoral research associate at the Department of Electrical and Computer Engineering, University of Manitoba, Canada. She received her PhD degree from King Abdullah University of Science and Technology (KAUST). She is a Senior member of IEEE and registered Professional Engineer in the province of Ontario, Canada. She is the founding chair of a special interest group on THz communications in

IEEE Communications Society (ComSoc) - Radio Communications Committee (RCC). She has been recognized as an Exemplary Reviewer (Top 2% of all reviewers) by IEEE Transactions on Communications in 2015, 2016, 2017, 2019, and 2020. She has been recognized as an Exemplary Editor by IEEE Communications Letters, 2020. Currently, she is serving as an Associate Editor in IEEE Communications Letters, IEEE Transactions on Green Communications, IEEE Communications Surveys and Tutorials, and IEEE Open Journal of Communications Society. Her research interests include stochastic modeling and optimization of wireless networks including vehicular, aerial, and satellite networks, millimeter and terahertz communication networks, machine learning empowered resource allocation in wireless networks.